

# Nanohybridized Synthesis of Metal Nanoparticles and Their Organization

Kensuke Naka and Yoshiki Chujo

## 1.1 Introduction

Metal nanoparticles have various unusual chemical and physical properties compared with those of metal atoms or bulk metal due to the quantum size effect and their large superficial area, which make them attractive for applications such as optics, electronics, catalysis, and biology [1, 2]. The catalytic properties of metal nanoparticles have generated great interest over the past decade. Among various metal nanoparticles, gold nanoparticles have tremendously high molar absorptivity in the visible region. Particle aggregation results in further color changes of gold nanoparticles solutions due to mutually induced dipoles that depend on interparticle distance and aggregate size. This phenomenon can be applied to various sensing systems [3–7]. The assembly of gold, silver, or copper nanoparticle monolayers is one of the ideal substrate for surfaced-enhanced Raman scattering (SERS) [8, 9].

Bare metal nanoparticles are prepared by employing physical methods such as mechanic subdivision of metallic aggregates and evaporation of a metal in a vacuum by resistive heating or laser ablation. Chemical methods such as the reduction of metal salts in solution are the most convenient ways to control the size of the particles and modified the surface chemical composition. To exploit nanoparticle properties for future device fabrication, self-organization of nanoparticles in a controlled manner is required. To construct such devices, new fabrication techniques must be developed with suitable metal nanoparticle-based building blocks. Several patterns for self-assemblies of the metal nanoparticles are schematically illustrated in Fig. 1.1.

A number of outstanding reviews on the synthesis and assembly of metal nanoparticle-based building blocks have appeared [2, 10]. This chapter highlights recent fabrication techniques of hybrid metal nanoparticles by controlled self-organization of the metal nanoparticle-based building blocks. Design of nanoparticle hybrids will be first focused on using building blocks for further assemblies. Several recent efforts have been concentrated on a system that

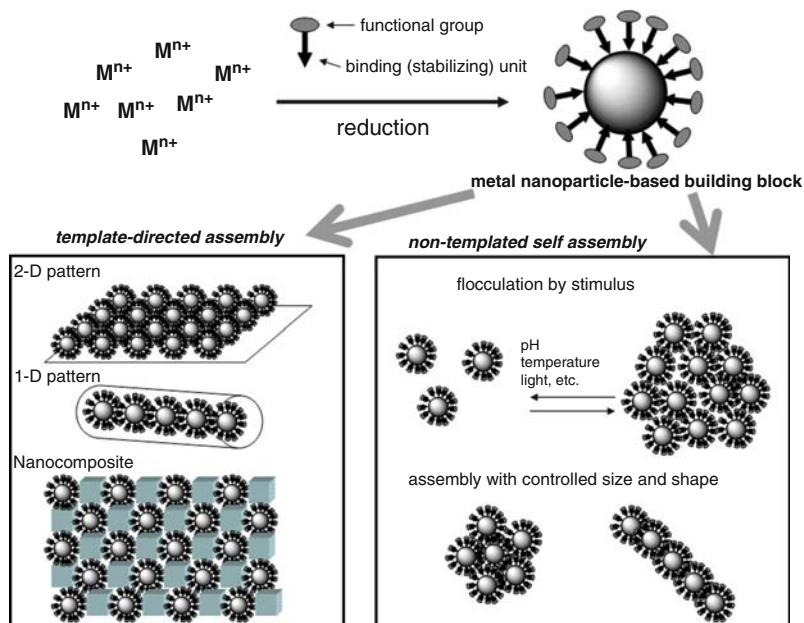


**Fig. 1.1.** Preparation of metal nanoparticle-based building blocks and their utilization for bottom-up nanofabrication

involves metal nanoparticles and dendritic molecules such as dendrimers and cubic silsesquioxanes. The organization of metal nanoparticles in superstructures of desired shape and morphology by using the dendritic molecules will be the main topic of this chapter. Several examples will also be described for the metal nanoparticles with various kinds of stimuli-responsive property, which involves aggregation or flocculation of metal nanoparticles in solution.

## 1.2 Design of Nanoparticle-Based Building Blocks

To exploit nanoparticle properties for future device fabrication by a “bottom-up method,” fundamental and key challenge is the design of the nanoparticle-based building blocks. From a synthetic chemical viewpoint, these metal nanoparticles required to be functionalized with a wide variety of organic moieties using simple chemical process. The most important requirement for this purpose is that repeatedly isolated and redissolved in common solvents, and handle and characterize as usual molecules. The metal nanoparticles can be stabilized by solvents or ions (Fig.1.2). Although they are eventually useful for catalysis, they tend to irreversibly aggregate over time or when removed from the solvent. To prevent the agglomeration, metal nanoparticles are protected by polymers which have coordination properties for the

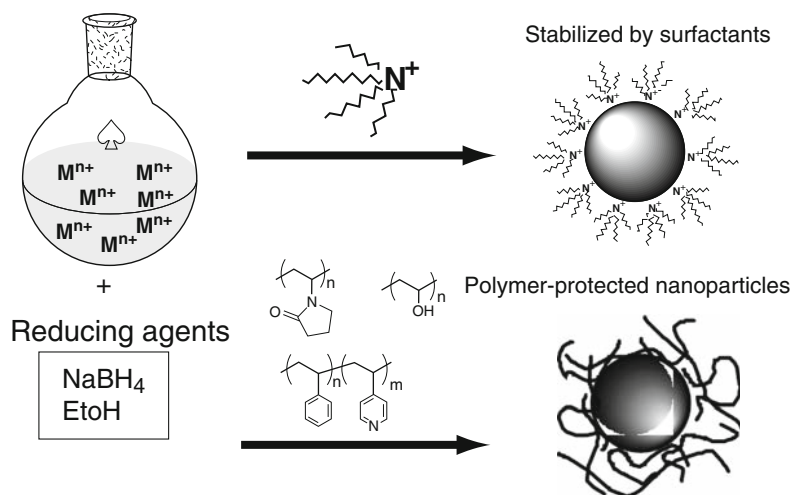


**Fig. 1.2.** Preparation of metal nanoparticles by chemical reduction in the presence of cationic surfactants (a) and polymers (b)

metal surfaces that are usually prepared as colloidal forms by reduction of metal ions in the presence of polymeric stabilizers such as poly(vinyl alcohol), poly(vinylpyrrolidone), and poly(vinyl ether) (Fig. 1.2) [11, 12]. Although these polymer-stabilized metal nanoparticles are stable in solution and easily prepared, requirement of large amount of polymers to stabilize metal nanoparticles inhibits close-packed assembly of the metal cores. Close-packed assembly of the metal nanoparticles is expected to produce complex electronic and functions based on quantum mechanical coupling of conduction electrons localized in each nanoparticle [13, 14]. Stabilization of metal nanoparticles by ligands as capping agents can enable further manipulation, control solubility characterization, and facilitate their analysis. Examples of ligand-stabilized metal nanoparticles are overviewed in the following sections.

### 1.2.1 Stabilized by Thiol Ligand

Mercapto groups (RSH) have been used as stabilizers of metal nanoparticles, especially for gold, in recent years, since Brust and coworkers [15] reported the preparation of ligand-stabilized gold nanoparticles by protecting the nanoparticles with a self-assembled monolayer of dodecanethiolate (Fig. 1.3). In this method (the Brust–Schiffrin method),  $AuCl_4^-$  is transferred from aqueous phase to toluene using tetraoctylammonium bromide as a phase-transfer reagent and then reduced by  $NaBH_4$  with alkanethiols, yielding nanoparticles having average core diameters in the range of 2–8 nm. The size of the resulting gold nanoparticles decreases with increasing thiol/ $HAuCl_4$  reaction molar ratio. The crude product is modestly polydisperse, but can be separated into rather monodisperse samples by fractional

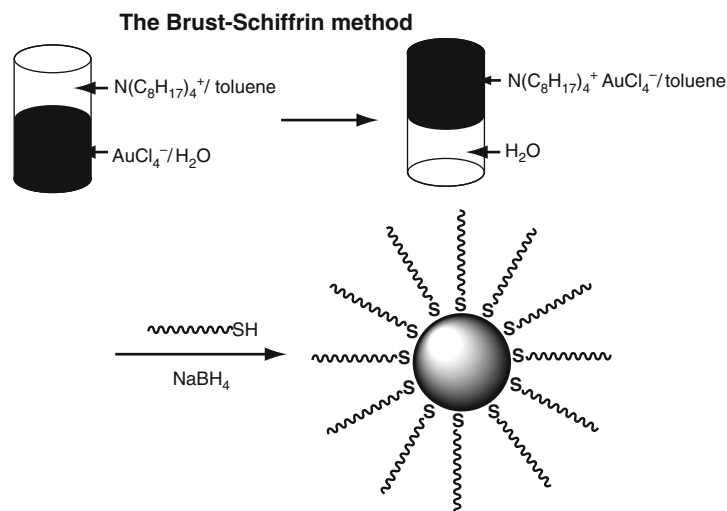


**Fig. 1.3.** Preparation of gold nanoparticles protected with monolayer of alkanethiols by two-phase method (the Brust-Schiffrin method)

precipitation. These monolayer-protected gold nanoparticles are repeatedly isolated and redissolved in common organic solvents such as toluene, hexane, and dichloromethane without irreversible aggregation or fusion. They are easy to handle and characterize just as stable organic compounds do. Monolayer-protected silver and palladium nanoparticles can also be prepared by the same protocol [14, 16].

Based on this system, efficient strategies to functionalize the metal nanoparticles have been developed. Murray et al. [17, 18] reported that surface functionalization can be achieved by simple place-exchange reactions of the alkanethiol monolayer-protected metal nanoparticles with  $\omega$ -functionalized alkanethiolates (Fig. 1.4). The rate and equilibrium stoichiometry are controlled by factors that include the reaction feed mole ratio as the equation shown in Fig. 1.4. Alternatively,  $\omega$ -functionalized alkanethiolates and dialkyl disulfides can be directly employed instead of alkanethiols as the same protocol in a single phase system [1].

The alkanethiolate monolayer-protected nanoparticles are insoluble in water, and while the place-exchanged nanoparticles bearing polar  $\omega$ -functionalities dissolve in several polar solvents, none has proven to be water soluble. Murray et al. [19] prepared water-soluble gold nanoparticles stabilized by a water-soluble tiopronine which can be repeatedly isolated and redissolved. Sodium (3-mercaptopropionate) (MPA)-stabilized gold nanoparticles were successfully prepared by citrate reduction of  $\text{HAuCl}_4$  in the presence of MPA. Simultaneous addition of citrate and MPA is essential to obtain their stable dispersions. The size of the particles can be controlled by the ratio of MPA/gold [20].

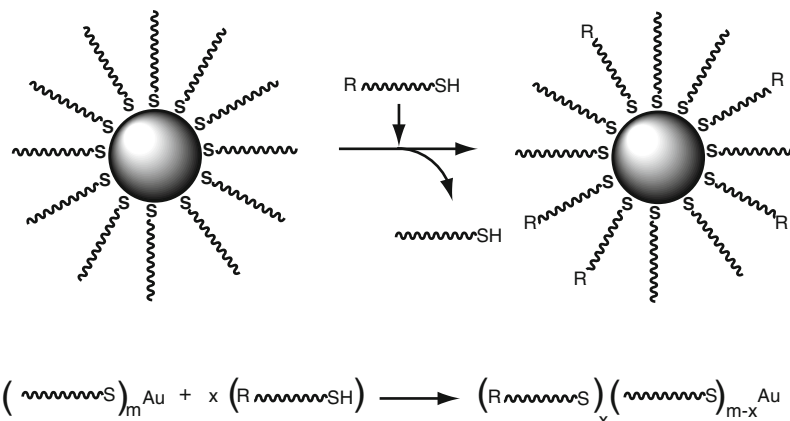
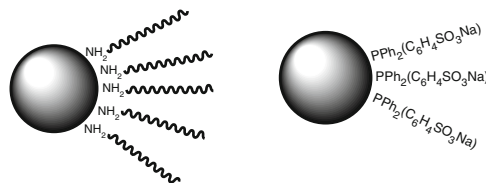


**Fig. 1.4.** General scheme for the place-exchange reaction between alkanethiol monolayer-protected gold nanoparticles and various functional thiols. In the bottom scheme,  $x$  and  $m$  are the number of new and original ligands, respectively

### 1.2.2 Stabilized by Amine Ligands

The Brust method of nanoparticle synthesis can be applied to generate amine-stabilized nanoparticles by simply substituting an amine for the thiol ligands (Fig. 1.5). Leff et al. [21] demonstrated that 2.5–7.0 nm average diameter gold nanoparticles can be stabilized by *n*-alkylamines. Jana and Peng [22] reported the synthesis of monodispersed gold, silver, copper, and platinum nanoparticles in a single organic phase. Although amines form only weakly bound and chemically unstable monolayers on bulk gold surfaces, the amine-capped nanoparticles are nearly as stable as their thiol-capped counterparts. Hiramatsu and Osterloh [23] reported a method for a large-scale synthesis of organoamine-protected gold and silver nanoparticles in 6–21 nm for Au and 8–32 nm for Ag size ranges and with polydispersities as low as 6.9%. The organoamine-protected gold nanoparticles of variable sizes formed by refluxing a solution of tetrachloroauric acid and oleylamine in toluene over the course of 120 min. The reducing equivalents in the reaction are provided by the amine, which can undergo metal ion-induced oxidation to nitriles. The weakly absorbed oleylamine on the nanoparticles can be readily displaced with aliphatic thiols by adding a solution of the oleylamine-ligated gold nanoparticles in toluene to a boiling solution of 5–10 equivalents (based on gold) of the thiol in the same solvent. Thiol-capped silver nanoparticles are obtained analogously at room temperature in chloroform. Aslam et al. [24] reported the synthesis of water-soluble gold nanoparticles with core diameters of 9.5–75 nm via reducing tetrachloroauric acid by oleylamine in water.

### Stabilized by Amines and Phosphines



### Stabilized by Bipyridyl Ligands

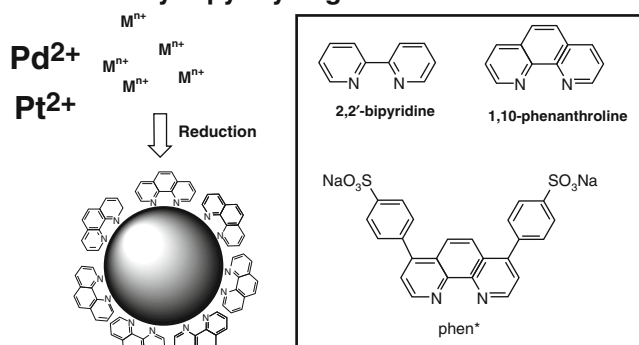


**Fig. 1.5.** Examples for ligand-stabilized metal nanoparticles prepared by reduction of metal ions in the presence of amine, phosphine, and bipyridyl ligands

#### 1.2.3 Stabilized by Bipyridyl Ligands

Ligand-stabilized metal nanoparticles with bipyridyl derivatives were reported as a simple method to protect colloidal particles with skin of ligand molecules which are not removed by isolation and are completely dry (Fig. 1.5) [25–29]. Palladium(II) acetate can be reduced in acetic acid solution by 1 atom hydrogen at room temperature with 2,2'-bipyridine or 1,10-phenanthroline, followed by  $O_2$  treatment [26]. Water-soluble, air-stable platinum nanoparticles were synthesized by stirring an acetic acid solution of platinum(II) acetate with 1,10-phenanthroline-4,7-bis(benzene-4-sulfonate) disodium salt (phen\*) [28].

#### 1.2.4 Stabilized by Phosphine Ligands

Phosphine-stabilized gold nanoparticles, originally formulated as  $Au_{55}(PPh_3)_{12}Cl_6$  by Schmid et al. [30] have been widely studied as models for metallic catalysts and precursors to other functionalized nanoparticle building blocks possessing well-defined metallic cores. Stable gold colloids stabilized by phosphines became available if  $HAuCl_4$  was reduced by trisodium citrate and treated with an excess of  $PPh_2(C_6H_4SO_3Na-m)$  or better  $P(C_6H_4SO_3Na-m)_3$ , which can be isolated by concentration of dilute solutions and addition of ethanol [25]. Since the phosphine is easily oxidized in air, the synthesis has to be carried out in an inert atmosphere. Palladium and platinum colloids

can be prepared by analogous procedures. Hutchison et al. [31] reported a convenient synthesis of 1.5 nm average diameter triphenylphosphine-stabilized gold nanoparticles. The phosphine-stabilized gold nanoparticles undergo rapid exchange of capping ligand phosphine with dissociated and added phosphine in dichloromethane solvent at room temperature [32]. Ligand exchange reactions of triphenylphosphine-stabilized nanoparticles with  $\omega$ -functionalized thiols provides a versatile approach to functionalized, 1.5 nm gold nanoparticles from a single precursor [33–35].

### 1.2.5 Controlling Numbers of Functional Group on Nanoparticle Building Blocks

To fabricate more complex assemblies comprising nanoparticle building blocks, controlling the number of functional groups on a metal nanoparticle surface is required. Two groups reported synthesis of monofunctionalized gold nanoparticles by using peptide synthesis protocols (solid-phase reaction) [36,37]. The key point of this method is the low-density packing of functional groups present in many solid-phase supports. Each functional group on a common polystyrene Wang resin bead possesses a rough volume of at least ca.  $9\text{ nm}^3$  when suspended in DMF, and thus a nanoparticle with a diameter smaller or around 2 nm can be loaded on the solid phase through a single bond per particle. Direct evidence of monofunctionalization is revealed by dimerization of the isolated gold nanoparticles, which were treated by a slow addition of ethylenediamine as a bridging linker in the presence of a condensation reagent. TEM images demonstrated that the dimer species are dominant and that 55–66% of particles on the TEM grid are found to undergo dimerization.

Dimers are of special interest because of their application as substrates in surface-enhanced Raman spectroscopy (SERS). Although the above approach is limited to very small particles, Shumaker-Parry et al. [38] synthesized gold nanoparticle dimers by a solid-phase approach using a simple coupling reaction of asymmetrically functionalized particles. Although a single functional group was not formed on a metal nanoparticle surface here, this method can be used to generate dimers with a wide size range and containing two nanoparticles with different sizes.

With a single functional group attached to the surface, such nanoparticles can be treated and used as molecular nanobuilding blocks to react with other chemicals to form nanomaterials with all the nanoparticle building blocks linked together by covalent bonding. Huo et al. [39] reported synthesis of a “nanonecklace” from monofunctionalized gold nanoparticles and polylysine by using an activated reagent in a solution. Goodson III et al. examined the nature of the electromagnetic coupling and its influence on nonlinear properties of Au-necklace particles with the aid of time-resolved spectroscopy and they found the presence of strong electromagnetic coupling between the neighboring particles [40].

Stellacci et al. [41,42] showed that mixtures of thiolated molecules formed ordered alternating phase when assembled on surfaces of nanoparticles. These

types of domains will profoundly demarcate the two diametrically opposed singularities at the particle poles. In the case of a self-assembled ligand shell, the polar singularities manifest themselves as defect points, i.e., sites at which the ligands must assume a nonequilibrium tilt angle. Ligands at the poles should be the first molecules to be replaced in the place-exchange reactions. Gold nanoparticles coated with a binary mixture of 1-nonanethiol and 4-methylbenzenethiol were prepared. To place-exchange at the polar defects, the gold nanoparticles were dissolved in a solution containing 40 molar equivalent of 11-mercaptoundecanoic acid (MUA) activated by *N*-hydroxysuccinimide [43]. A two-phase polymerization reaction was performed by combining a toluene solution containing the MUA-functionalized nanoparticles with a water phase containing divalent 1,6-diaminohexane. A TEM image of a precipitate formed at the water-toluene interface showed a large population of linear chains of nanoparticles. The chains were soluble in dichloromethane and showed a film-forming property.

### 1.3 Well-Defined Nanoparticle Hybrids with Linear Polymers

#### 1.3.1 Polymer-Grafted Metal Nanoparticles

Construction of well-defined polymers containing metal nanoparticles is one of the attractive targets for polymer and material chemistry and would become nanoparticle-based building blocks for further fabrication toward nanodevices. To connect a polymer end with a surface of metal nanoparticle, covalent and coordination bonds are considered to be the most suitable links as a similar concept as the numerous reports on the metal nanoparticles functionalized with the low molecular weight ligands. Attachment of metal nanoparticles to synthetic polymers adds film-forming properties to the metal nanoparticles and also provides the opportunity for microphase separation between the metal nanoparticles and the polymer matrix. The pioneer work in this field has been explored by Mirkin et al., who introduced a strategy for covalent attachment of DNA strands to gold nanoparticles [6].

A polymer-grafted metal nanoparticle was produced by reduction of metal ion with a bipyridyl-terminated polymer (Fig. 1.6) [44]. As described in Sect. 1.2.3, the bipyridyl ligands stabilized palladium and platinum nanoparticles were simply prepared and the ligand molecules were not removed even after isolation and drying. The palladium nanoparticles were synthesized by stirring an acetic acid solution of palladium(II) acetate and bipyridyl-terminated poly(oxyethylene) (bpy-POE) (MW = 2,000) (molar ratio 8:1) under 1 atm hydrogen at room temperature. After isolation, the polymer-grafted metal nanoparticles became soluble in various solvents such as CH<sub>2</sub>Cl<sub>2</sub>, CHCl<sub>3</sub>, MeOH, acetone, and water. The solubility of the resulting nanoparticles was the same as that of poly(oxyethylene). These solutions were stable



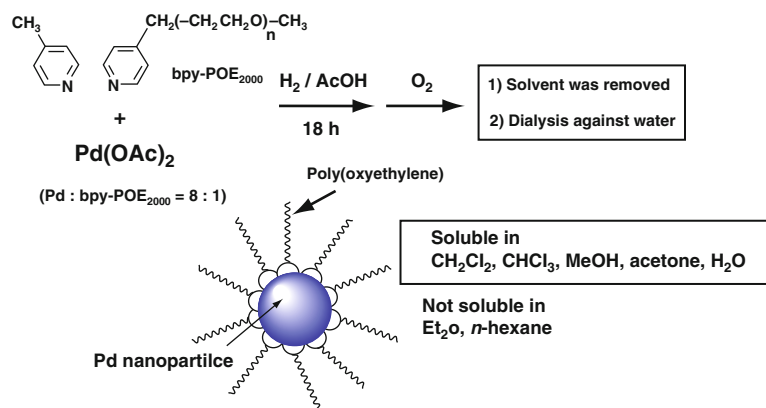


**Fig. 1.6.** Polymer-grafted palladium nanoparticles prepared by reduction of metal ions with  $\text{H}_2$  in the presence of a bipyridyl-terminated poly(oxyethylene)

for more than half a year at room temperature under air. Although the formation of palladium nanoparticles was reported when an acetic acid solution of palladium(II) acetate was stirred with a large excess amount of poly(ethylene oxide) (MW = 900,000) under 1 atm hydrogen at room temperature, extremely larger amounts of the polymer (molar ratio 1:10) were required and the precipitation of the metal occurs after a comparably short time (1–2 days) [45].

Murray and coworkers [46] reported that a thiolated polymer,  $\alpha$ -methoxy- $\omega$ -mercapto-poly(ethylene glycol) (PEG-SH, MW = 5,000), was used to produce polymeric monolayer-protected gold nanoparticles. The PEG-SH ligand was also selected because of the dissolution of  $\text{LiClO}_4$  electrolyte. Thus, the resulting nanoparticles can be applied for new polymer electrolyte media, a semisolid having an ionically conductive nanophase around a metallic core. Thiol-functionalized poly(acrylamides) were also attached on the surfaces of metal nanoparticles [47, 48].

Gold nanoparticles grafted with hydrophobic homopolymer chains such as thiol-capped polystyrenes were prepared [49]. Kramer and Pine [50] reported about gold nanoparticles coated with a mixture of two different polymeric thiols, which created an amphiphilic shell as suggested by the observed accumulation of particles at the interface separating the domains of polystyrene and poly(2-vinylpyridine). Zubarev et al. [51] reported an efficient method to produce amphiphilic gold nanoparticles with an equal number of hydrophobic and hydrophilic arms. They used a V-shaped polybutadiene–poly(ethylene glycol) amphiphile containing a functional group at its junction point.

A more promising approach for the preparation of covalently attached polymer is given by the use of immobilized initiators for the in situ generation of the grafted polymer, which is the so-called a “grafting-to” method. This method can be applied for a variety of monomers utilizing radical, cationic, and anionic polymerization. To obtain a homogeneous grafted polymer, first

the surface grafting density has to be uniform, second the polydispersity index should be near 1, and finally all chains should be linear. These requirements are achieved by living polymerization. Fukuda and coworkers [52] reported synthesis of gold nanoparticles coated with well-defined, high-density polymer brushes by surface-initiated living radical polymerization. The “grafting-to” method applied for poly(methyl methacrylate) shells by surface-confined living radical polymerization [53], a thermoresponsive polymer by surface-induced reversible-addition-fragmentation chain-transfer polymerization [54], and ring-opening polymerization of lactones [55]. Palladium nanoparticles with surface initiators for ring-opening polymerization of 2-methyl-2-oxazoline were prepared by alcohol reduction method of palladium(II) acetate in the presence of a bipyridyl ligand [56].

### 1.3.2 $\pi$ -Conjugated Polymer Metal Nanoparticle Hybrids

Composites of metal nanoparticles and  $\pi$ -conjugated polymers are useful for several applications [57]. Incorporation of metal nanoparticles enhances conductivity of the polymers [58]. The electronic structure of the polymer chain strongly influences the characteristic of embedded metal nanoparticles [59,60]. These composites have potential as catalysts since the  $\pi$ -conjugated polymer might provide a potentially efficient route for shuttling of electronic charge to the catalytic centers [61,62]. If  $\pi$ -conjugated polymers have strong electron-donating properties, reduction of metal ions occurs via the electron transfer from the  $\pi$ -conjugated polymers to the metal ions, leading to the formation of metal nanoparticles. Polymers having reducing as well as stabilizing abilities would provide “clean” materials because the additional reducing agent would not be necessary. Huang and coworkers have reported about the simultaneous in situ reduction of metal ions, palladium(II) and gold(III), to their elemental forms, which, however, were not dispersed in most common solvents [63–65].

$\pi$ -Conjugated polymer-protected gold, palladium, and platinum nanoparticles of narrow size distribution in stable colloidal form were prepared via reduction of each metal salt by a  $\pi$ -conjugated poly(dithiafulvene) (PDF) having electron donating properties (Fig. 1.7) [66,67]. A series of  $\pi$ -conjugated PDFs have been prepared by cycloaddition polymerization of aldothioketenes and their alkanethiol tautomers, which were derived from aromatic diynes [68]. Reduction of metal ions by the  $\pi$ -conjugated polymer forms metal nanoparticles and the resulting oxidized polymer protected the metal nanoparticles. The resulting DMSO solution of the polymer-protected gold nanoparticles was stable without precipitation for more than a month at room temperature under air. Due to the effective expansion of  $\pi$ -conjugation of PDF by charge transfer, the absorption spectrum of the oxidized PDF showed a red-shift compared with that of the neutral PDF. The palladium nanoparticle dispersed  $\pi$ -conjugated PDF exhibited an anodic shift of oxidation potential for the dithiafulvene (DF) unit compared with that in the neutral PDF.

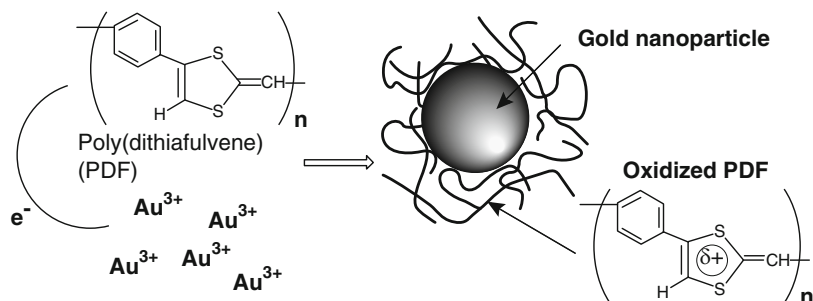


**Fig. 1.7.** Formation of  $\pi$ -conjugated poly(dithiafulvene) (PDF)-protected metal nanoparticles via reduction of metal ions by the  $\pi$ -conjugated electron-donating PDF

The oxidized polymer with delocalized positive charges provided both steric and electrostatic stabilization, protecting the metals as stable colloidal forms.

Polymers having pendant reducing groups were used to prepare metal nanoparticles, in which the additional step of introducing a reducing agent would not be necessary. Henpenius et al. [69] prepared gold nanoparticles inside polystyrene–oligothiophene–polystyrene triblock micelles in toluene without additional reducing agents. Gold nanoparticles were produced in aqueous solutions by a polyelectrolyte that possesses pendant terthiophene derivatives as the reducing group for  $\text{HAuCl}_4$  [70]. Polysilane shell-crosslinked micelles, where the polysilane core is surrounded by a partially crosslinked shell of poly(methacrylic acid), can be used as the template for the synthesis of metal nanoparticles [71].

## 1.4 Organization of Metal Nanoparticles

### 1.4.1 Overview of Metal Nanoparticle Organizations

The realization of technologically useful nanoparticle-based materials depends not only on the quality of the nanoparticles (e.g., size and shape) but also on their spatial orientation and arrangement. The building and patterning of the metal nanoparticles into organized structures is a potential route to chemical, optical, magnetic, and electronic devices with useful properties [72–74]. Fabrication of nanoparticles into one-, two-, and three-dimensional structures is an attractive, challenging target for developing bottom-up nanofabricate techniques, since the collective properties of the resulting structures are expected to be different from those of the corresponding isolated nanoparticles [75, 76]. The development of practical strategies for the assembly of metal nanoparticles into order structure is thus an area of considerable current interest. The organization of metal nanoparticles in superstructures of desired shape and

morphology is a challenging research area. Various strategies such as solvent evaporation [77, 78], electrostatic attraction [79], hydrogen bonding [80–82], DNA-driven assembly [5], and crosslinking induced by organic molecules [83] have been developed to form nanoparticle assemblies. Rotello et al. [84] have shown many excellent fabrication techniques to utilize polymers for controlled assemblies of metal nanoparticles.

Especially, the assembly of metal nanoparticles on solid supports has attracted substantial research efforts as a consequence of their unique electronic and optical properties [85–88]. For example, colloidal gold and silver nanoparticles are excellent building blocks for surface-enhanced Raman scattering-active substrates [89, 90]. Different techniques, including Langmuir–Blodgett technique and electrophoretic deposition technique [91–94] have been used to obtain two-dimensional assembling of metal nanoparticles. One of the efficient methodologies for the organization involves the utilization of electrostatic interaction between a substrate and metal nanoparticles [95–98]. Schmitt et al. reported layered nanocomposite films prepared from colloidal metal nanoparticles through electrostatic interaction. Most successful routes required the surface modification of a solid substrate by positively charged polyelectrolytes because of the negatively charged metal nanoparticles.

The organization of metal nanoparticles in 1D assembly has met with limited success compared with 2D and 3D assemblies. Most of the successful methods required appropriate templates. Schmid and coworkers [99, 100] used ordered channels of porous alumina as a template to obtain linear arrangements of gold nanoparticles. The utilization of structured carbon and alumina substrate as a template also has been reported [101–103]. Teranishi and coworkers [101] reported the fabrication of one-dimensional arrangement of size-controlled gold nanoparticles in combination with a nanoscale ridge-and-valley structured substrate. Biological macromolecules have been used to build defined inorganic nanostructures. Among the biological macromolecules, DNA is one of the most interesting templates because of its diameter of only 2 nm and the micrometer-long distribution of well-defined sequence of DNA bases. Several papers reported the fabrication of one-dimensional arrangement templated by DNA [104–111]. Other biological materials such as peptide, virus, lipid, and biopolymers were also used [112–115]. The most important advantage of using biological materials is their single molecular weights, which provide controlled length of one-dimensional arrays. Nonbiological templates such as carbon nanotubes and polycation molecules templated self-assembly of gold nanoparticles also have been reported [116–118].

A scanning probe lithography technique, “dip-pen” nanolithography, has demonstrated the ability to pattern the metal nanoparticles with sub-100 nm resolution on substrates [119–121]. To draw a familiar analogy, the AFM tip acts as a “pen,” the organic or inorganic molecules act as “ink,” and the surface acts as a “paper” for nanostructures to be “drawn” on.

### 1.4.2 Organization of Metal Nanoparticles by Dendritic Molecules

This section will highlight the organization of metal nanoparticles by using dendritic molecules with 3D, 2D, and 1D arrangements. Dendrimers are monodisperse macromolecules with a regular and highly branched 3D architecture. The starburst structures are disk-like shapes in the early generations, whereas the surface branch cell becomes substantially more rigid and the structures are spheres [122]. Dendrimers have been attracting much attention as useful stabilizers of metal nanoparticles in solution, since the first successful report by Crooks and his coworkers in 1998 [123]. Most of these studies deal with the reduction in a solution where dendrimers are molecularly dissolved, essentially isolated from one another in solution, and metal ions are encapsulated in the interior space of the single dendrimer. The ions are reduced to metal atoms which self-assemble into a metal nanoparticle within the single dendrimer. Colloidal forms of gold nanoparticles in the 2–3 nm size regime were prepared by in situ reduction of  $\text{HAuCl}_4$  in the presence of amine-terminated poly(amidoamine) (PAMAM) dendrimers [124–127]. The dendrimers operate as a very effective protective colloid for the preparation of gold particles since only a very small amount of the dendrimers is required to obtain nanometer size of gold particles compared to other linear polymers. Transmission electron microscopy (TEM) and dynamic light scattering (DLS) data suggested that the dendrimers adsorbed on the gold nanoparticles as a monolayer [127]. The driving force for the interaction of the metal nanoparticles with the dendrimers is an association of gold with the primary amine terminal groups and the interior secondary and tertiary amines (especially for early generations). The resulting dendrimer/gold nanocomposites can be isolated from alcohol/water solutions by precipitation with tetrahydrofuran (THF) [126]. The required concentration is large in the case of weak interaction between platinum nanoparticles and dendrimers with amino groups [125].

Cubic silsesquioxanes are also regarded as the dendritic molecules for self-organization of metal nanoparticles. Octa(3-aminopropyl)octasilsesquioxane octahydrochloride (OAPOSS) is regarded as a structure equivalent of the G1.0 PAMAM dendrimer. In contrast to the PAMAM dendrimer, OAPOSS has an inner cubic rigid inorganic core with the size of 0.5 nm containing silicon and oxygen, which offers uniform interparticle spacing, good thermal and mechanical properties, and solvent resistance. Since the cubic silica core is rigid, the eight organic functional groups of OAPOSS are appended to the vertexes of the cube via spacer linkage [128, 129]. Although the structure of the G1.0 PAMAM dendrimer is a disk-like flexible random shape, the functional groups of OAPOSS should become more rigid and the structure is spherical [130]. In contrast to the synthesis of the dendrimers, OAPOSS is simply prepared and isolated as precipitates by hydrolysis of aminopropyltriethoxysilane in an aqueous acidic methanol [131, 132].

The OAPOSS-protected gold nanoparticles were prepared through reduction of  $\text{HAuCl}_4$  in the presence of OAPOSS by  $\text{NaBH}_4$  [133]. The size of

the resulting gold nanoparticles increased with the increase in the  $\text{HAuCl}_4/\text{OAPOSS}$  molar ratio. The OAPOSS-protected gold nanoparticles with a diameter of 80 nm can be prepared at the  $\text{HAuCl}_4/\text{OAPOSS}$  molar ratio of 20. The OAPOSS-protected gold nanoparticles were assembled effectively on a slide glass [132]. The glass was immersed in the aqueous solution of the OAPOSS-protected gold nanoparticles. After the immersion, the glass was washed with  $\text{H}_2\text{O}$  several times to remove extra gold nanoparticles. An absorbance feature of the glass at 537 nm indicated the adsorption of the OAPOSS-protected gold nanoparticles. The absorbance continually increased with increasing the immersion time. The surface plasmon band was gradually redshifted from 525 to 566 nm. This is a consequence of overlap of the dipole resonances between neighboring gold nanoparticles on the glass substrate. That is, as the particle coverage increases, interparticle spacing becomes small compared to the incident wavelength. These results indicate that the gold nanoparticles have a positive charge and were immobilized densely on the glass substrate.

One of the efficient methodologies for the organization of 3D arrangement involves the utilization of chemical crosslinking by organic ligands. However, the combination of the metal nanoparticles with bifunctional linking molecules having rigid or flexible structures usually results in the formation of insoluble and uncontrollable aggregates in solutions. Unlike a bifunctional linker, stronger bonding of the dendritic molecules to the inorganic surfaces is expected due to a chelate or cluster effect. Rotello and coworkers [134] employed PAMAM dendrimers of different generations to both assemble gold nanoparticles and control the separation distance between them. In this system, the gold nanoparticles were functionalized with carboxylic acid terminal groups. Salt-bridge formation between the dendrimer surface-amine groups and the nanoparticle peripheral carboxylic acid groups led to electrostatic self-assembly between the dendrimer and nanoparticle component.

Chujo and Naka [135] reported an assembling of metal nanoparticles into spherical aggregates as colloidal forms in solution via self-organized spherical templates in a solution by using dendritic molecules such as OAPOSS- or amine-terminated PAMAM dendrimers (Fig. 1.8). When a methanol solution of OAPOSS and palladium(II) acetate was stirred at room temperature, the solution immediately became turbid, which suggested aggregate formation. The turbid solution gradually turned from yellow to black with an increase in the reaction time, indicating the reduction of the palladium ions. One drop of the turbid solution containing the obtained product was placed on a copper grid and allowed to evaporate the solvent under atmospheric pressure at room temperature. TEM showed that the spherical aggregates with a mean diameter of 70 nm were obtained (Fig. 1.8). These spherical aggregates were clearly composed of dark spots. These dark spots were individual palladium nanoparticles. Every nanoparticles, with a size of  $4.0 \pm 0.8$  nm, appeared as a discrete entity in the nanosphere. Scanning electron microscopy (SEM) data also indicated the formation of spherical aggregates in size of  $80 \pm 20$  nm.

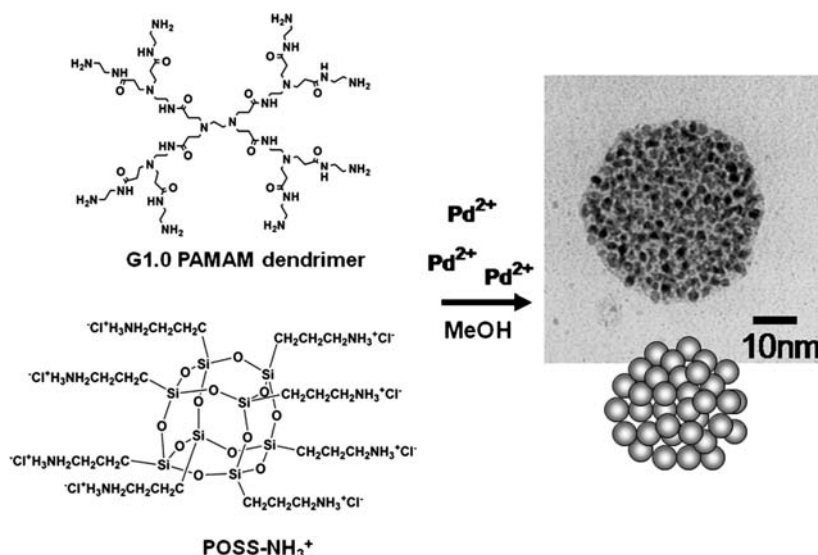


**Fig. 1.8.** Formation of spherical aggregates composed of palladium nanoparticles and the dendritic molecules (G1.0 PAMAM dendrimers or POSS-NH<sub>3</sub><sup>+</sup>) in methanol

The resulting black colloidal solution was stable and neither precipitated nor flocculated over a period of several months.

The highly ordered spherical aggregates were composed of palladium nanoparticles, in which the dendritic molecules acted as crosslinkers and stabilizers for palladium nanoparticles. Palladium nanoparticles are attractive materials for catalysis [136, 137] and hydrogen storage [137]. Building the nanoparticles into hierarchical structures with stable manner should be required for these applications. TEM observations suggested that the density of palladium nanoparticles in the aggregates using OAPOSS as a template is higher than those using the amine-terminated G1 PAMAM dendrimer. From a TM-AFM image, the shapes of the aggregates using OAPOSS and the amine-terminated G1 PAMAM dendrimer were an oval and a spherical form on the plate, respectively. Increasing rigidity of the core of the dendritic molecules increased stability of the spherical form in the dry state.

The reaction and reaction-induced self-assembling process were explored in situ by means of a combined time-resolved method of small angle neutron scattering and small-angle X-ray scattering [138]. The dendrimer molecules and palladium(II) acetate first self-assemble themselves rapidly into spherical aggregates and thereafter their size was kept almost constant. Inside the aggregates, which serve as a template for the reaction, the reduction of palladium(II) acetate to palladium(0) and their self-assembly into palladium nanoparticles proceeds gradually with time over 12 h. The formation of the spherical aggregates was also supported by TEM.



Effect of different generation of the PAMAM dendrimers for the structure of the aggregates was observed. Using the G0 PAMAM dendrimer instead of the G1.0 PAMAM dendrimer under the same condition resulted in the formation of uniform, spherical aggregates with a diameter of 50 nm composed of palladium nanoparticles. On the other hand, the G2.0 PAMAM dendrimer decreased the size of the spherical aggregates. Although the exact reason for these phenomena is not entirely clear, we speculate that these results would be due to the difference of the functionality of the PAMAM dendrimers structure. That is, in the case of higher the PAMAM dendrimers generation, stronger interaction between colloids would be expected due to increase of the functional groups.

Wire-like aggregates of palladium nanoparticles were self-organized in an acidic methanol solution by using the G1.0 PAMAM dendrimer (Fig. 1.9) [139]. The combination of the G1.0 PAMAM dendrimer and metal ions in solution formed wire-like colloids, which would act as spatially constrained template for controlled synthesis of the metal nanoparticles. It is worth pointing out

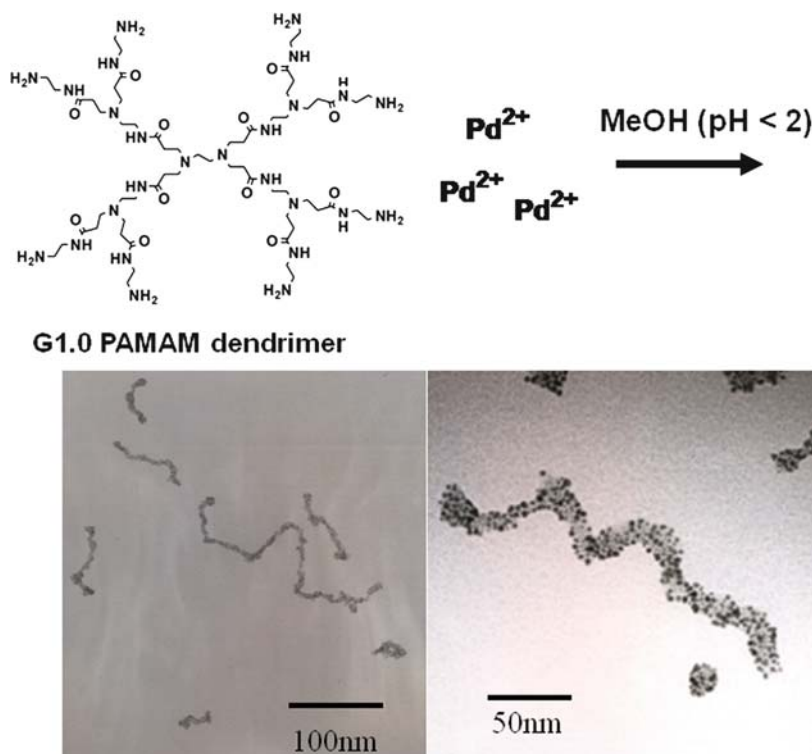


**Fig. 1.9.** TEM image (a) and magnified TEM image (b) of the wire-like aggregates of palladium nanoparticle with the G1 PAMAM dendrimers prepared in the acidic methanol solution. Scale bars of (a) and (b) are 500 and 100 nm, respectively



that the wire-like aggregates are formed spontaneously without any external force and templates. When the acidic methanol solution of the G1.0 PAMAM dendrimer and palladium(II) acetate was stirred at room temperature, the solution immediately became turbid. This suggests microscopic aggregate formation. The solutions gradually turned from yellow to black with increasing reaction time, indicating the reduction of palladium ions and the formation of palladium nanoparticles. One drop of the solution containing the obtained product was placed on a copper grid and allowed to evaporate the solvent under atmospheric pressure at room temperature. The TEM investigation showed the wire-like aggregates (Fig. 1.9). The length of most of the wire-like aggregates was more than  $0.5\text{ }\mu\text{m}$ . These wire-like aggregates were clearly composed of dark spots. These dark spots were individual palladium nanoparticles. Every nanoparticles with a size of  $4.0\pm 0.8\text{ nm}$ , appeared as a discrete entity in the aggregates. A SEM investigation also indicated that the obtained products were wire-like structure. DLS showed that the average hydrodynamic radius was around  $300\text{ nm}$  indicating the presence of the aggregates in the solution.

#### 1.4.3 Self-Organized Nanocomposites

A major challenge for nanoparticle-based nanocomposites is the preparation of thermally and mechanically stable nanocomposites with high content of metal nanoparticles and preventing both phase separation and aggregation of the metal nanoparticles in the host matrices. Several studies have been done on the self-organization of metal nanoparticles with monofunctionalized silsesquioxanes at a molecular level [100, 140]. Polyhedral octasilsesquioxane derivatives have strong tendency to crystallize. Rotello et al. [140] reported the formation of spherical aggregates with uniform internal spacing using diaminopyridine-functionalized polyhedral octasilsesquioxane and thymine-functionalized gold nanoparticles. Initially, there was the three points hydrogen bonding of the diaminopyridine unit with complementary thymine unit followed by subsequent aggregation and crystallization of the silsesquioxane moieties. Multifunctionalized cubic silsesquioxanes such as octa(3-aminopropyl)octasilsesquioxane (OAPOSS) were recently used to synthesize nanocomposites of metal nanoparticles. These types of cubic silsesquioxane provide alternative assemblies of functionalized metal nanoparticles. Rotello and coworkers [141] reported that electrostatic interaction between the carboxylic acid groups coated on gold nanoparticles and the ammonium groups on OAPOSS resulted into well-ordered nanocomposites featuring uniform interparticle spacings. Samples of electrostatically coupled nanoparticles were prepared by dropping solutions of carboxylic acid-functionalized gold nanoparticles in THF/MeOH into a solution of OAPOSS in MeOH/H<sub>2</sub>O.

The use of OAPOSS has additional important advantages. First, amide bonds were formed between the reaction ion couples well defined in nanocomposites during subsequent chemical reaction to generate nanocomposites with improved chemical properties. Second, calcination of the nanocomposites of

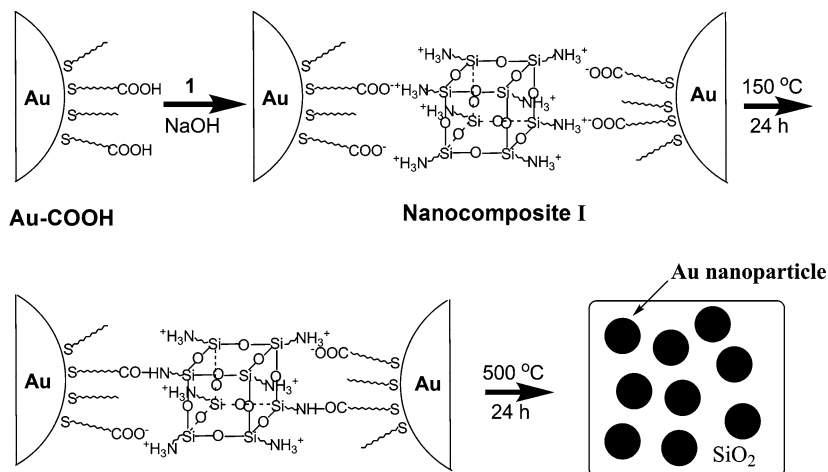


**Fig. 1.10.** Self-organized nanocomposites of functionalized gold nanoparticles with OAPOSS

the gold nanoparticles with OAPOSS would form silica-gold nanoparticle nanocomposites without the fuse of the gold nanoparticles, since the inorganic core of OAPOSS should be maintained by calcination on the contrast of organic linkers. Naka and Chujo [142] recently reported a self-organized nanocomposites of functionalized gold nanoparticles with OAPOSS via electrostatic interaction between the carboxylate anions and ammonium cations (Fig. 1.10). Subsequent chemical reaction between the reactive ion couples well defined in the nanocomposites generated amide bonds between the two components.

When a DMSO solution of OAPOSS and the carboxylic acid-functionalized gold nanoparticles (Au-COOH) was neutralized by an aqueous NaOH solution, the dark red solution faded completely and the gold nanoparticles precipitated out from the solution to form nanocomposite I (Fig. 1.10), which consisted of 11.0 wt% OAPOSS and 89.0 wt% Au-COO<sup>-</sup>, estimated by thermogravimetric analysis (TGA) and elemental analysis of N. Even a half amount of OAPOSS against Au-COOH was added into a DMSO solution of Au-COOH, the TGA results indicated that the resulting nanocomposite consisted of 11.3 wt% OAPOSS and 88.7 wt% Au-COO<sup>-</sup>, which was of the same composition as that of nanocomposite I. These results made it clear that the formed nanocomposites were not random aggregation between OAPOSS and Au-COO<sup>-</sup>. The TEM image of nanocomposite I showed the existence of gold nanoparticles with a size of  $6.0 \pm 2.4$  nm, which means no fuse of the gold nanoparticles occurred during the precipitation.

More stable nanocomposite II was produced after the nanocomposites I underwent a subsequent chemical reaction by heating at 150 °C for 24 h (Fig. 1.10). An absorption peak corresponding to -CONH- bonds at

$1,650\text{ cm}^{-1}$  appeared, indicating that amide bonds were formed between the well-defined reactive ion couples after the reaction. The average size of the gold nanoparticles in nanocomposite II was  $6.4 \pm 2.2\text{ nm}$ . Further heating of nanocomposite II at  $500^\circ\text{C}$  for 24 h resulted nanocomposite III in which the organic moiety of OAPOSS totally decomposed, and the inorganic cores of OAPOSS were maintained (Fig. 1.10) [143]. Generally, such a high heating temperature results in partial melting and interconnection between the gold nanoparticles [144]. The TEM image of nanocomposite III showed the existence of the gold nanoparticles with a size of  $7.0 \pm 2.5\text{ nm}$ . This suggests that no significant increase in particle size of the gold nanoparticles occurred even after the calcination at  $500^\circ\text{C}$  due to the rigid inorganic cores of OAPOSS.

The controlled organization of metal nanoparticles into multilayer films and porous nanocomposites has received intense attention in recent years for their uses in analytical and material chemistries, mainly because of their unique chemical and physical properties, which are different from those of bulk metals [2,8,9]. Self-assembled multilayer films of the metal nanoparticles have become a popular target in nanoscale material synthesis in the last few years [145] because they are complementary alternative to traditional preparation methods of metal films such as evaporation and plating. Self-assembled ultrathin multilayer films have been intensively investigated in recent years, since Decher et al. [146,147] introduced the method for preparing multilayer ultrathin films by the consecutive deposition of oppositely charged polyelectrolytes from dilute aqueous solution onto charged substrates. It was reported that a self-assembled multilayer poly(octadecylsiloxane) provided a nanostructured matrix for metal nanoparticle formation [148]. Silver nanoparticles stabilized by negatively charged polystyrene microspheres were transported into layer-by-layer (LBL) film structures via self-assembly between the microspheres and poly(ethyleneimine) [149]. The work of Natan and coworkers [150] is representative of a bifunctional crosslinker-directed stepwise construction of conductive gold and silver colloidal multilayers. Controllable and reversible self-assembled multilayer films of gold nanoparticles were also efficient based on ligand/metal ion/ligand linkers [151]. Vapor-sensitive multilayer films were obtained via a LBL self-assembly of gold nanoparticles and dendrimers [152].

Naka and Chujo [153] reported that the LBL self-assembled multilayer films were successfully prepared via the adsorption of a facile approach of immersing the negatively charged glass substrates into OAPOSS and  $\text{Au-COO}^-$  solutions alternatively. Electrostatic interaction between the  $-\text{COO}^-$  on  $\text{Au-COO}^-$  and the  $-\text{NH}_3^+$  of OAPOSS was the driving force of the LBL self-assembly in a manner similar to the one reported by Caruso and coworkers, in which they created nanocomposite siliceous thin films by the LBL self-assembly in alternation with octa(3-aminopropyl)octasilsesquioxane and poly(styrene-4-sulfonate) to form thin films on planar and spherical supports [21]. A linear increase of the surface plasmon resonance of  $\text{Au-COO}^-$  with the deposited bilayers indicates that each deposition cycle adds a virtually constant amount of  $\text{Au-COO}^-$  on the film in each dipping cycle.

A high content and dense coverage of the gold nanoparticles provide the LBL multilayer films with bulk gold appearance and relatively high conductivity.

Films' colors shifted from dark red to yellow. The surface plasmon resonance band responsible for the dark red color exhibited by the gold nanoparticles arises from interband transition between the highly polarizable Au 5d band and the unoccupied states of the conduction band [13]. The intensity of the plasmon band is related to the quantity of Au-COO<sup>-</sup> deposited on the substrate. The darkening of the dark red color reveals increasing content of the gold nanoparticles from 1-, 3-, 5-, to 10-bilayer films. After 15 exposures to the 1/Au-COO<sup>-</sup> dipping cycle, the 15-bilayer film had a final appearance similar to bulk gold in color and reflectivity, suggestive of bulk gold behavior. The same phenomena were observed by Natan and coworkers [150].

Recent years have focused much attention on self-assembly of the metal nanoparticles to generate porous nanostructures. The porous metal nanostructures have potential application in the areas of advanced catalysis, electronics, optics, separations, and sensors [154]. A facile method was proposed to incorporate preformed gold nanoparticles within ordered macroporous materials [155]. Porous structures with metal nanoparticles were also produced by cyclodextrin-assisted incorporation of metal nanoparticles into porous silica [156]. Silica and gold nanoparticles were cooperatively assembled with lysine-cysteine diblock copolypeptides into hollow spheres [157], as the copolypeptide provided preferential attachment sites for silica and the gold nanoparticles.

Porous nanocomposites were prepared by precipitation of OAPOSS modified polystyrene (PS), latex particles, and Au-COO<sup>-</sup> followed by removal of the PS particles via solvent extraction (Fig. 1.11). The OAPOSS-modified

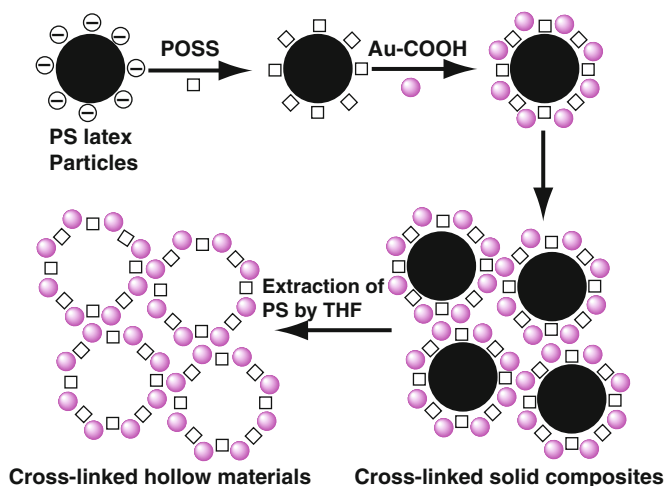


**Fig. 1.11.** Experimental procedures for preparation of porous nanocomposites by precipitation

PS latex particles precipitated out from the  $\text{Au-COO}^-$  solution after being crosslinked by  $\text{Au-COO}^-$ . The size of the gold nanoparticles was 3.0 nm estimated from the XRD pattern of the porous nanocomposites. After the porous nanocomposites underwent a subsequent chemical reaction by heating at  $150^\circ\text{C}$  for 24 h, an absorption peak corresponding to  $-\text{CONH}-$  bonds at  $1,650\text{ cm}^{-1}$  appeared in FT-IR spectra, indicating that amide bonds were formed between the well-defined reactive ion couples after the reaction, similar to the formation of nanocomposite II as shown in Fig. 1.10. The estimated size of the gold nanoparticles in the porous nanocomposites was also  $\approx 3.0\text{ nm}$ , calculated from the XRD pattern of the porous nanocomposites after the reaction. It was concluded that no size growth of the gold nanoparticles occurred during the chemical reaction. This strategy associated with the LBL self-assembly technique was applied here to prepare porous nanocomposites from the two components. Nanocomposite films with exactly spherical pores were produced by the LBL self-assembly of the OAPOSS-coated PS latex particles and  $\text{Au-COO}^-$  on the glass substrate. Figure 1.12 shows SEM images of the films after four dipping cycles before and after removal of the PS latex particles by solvent extraction or calcination at  $500^\circ\text{C}$ . The pore size and shape were intact after removal of the templates.

Physical and chemical crosslinking is an effective method of building and patterning nanostructures consisting of two or more types of nanoparticles with at least one type of metal nanoparticle. Incorporation of more than a

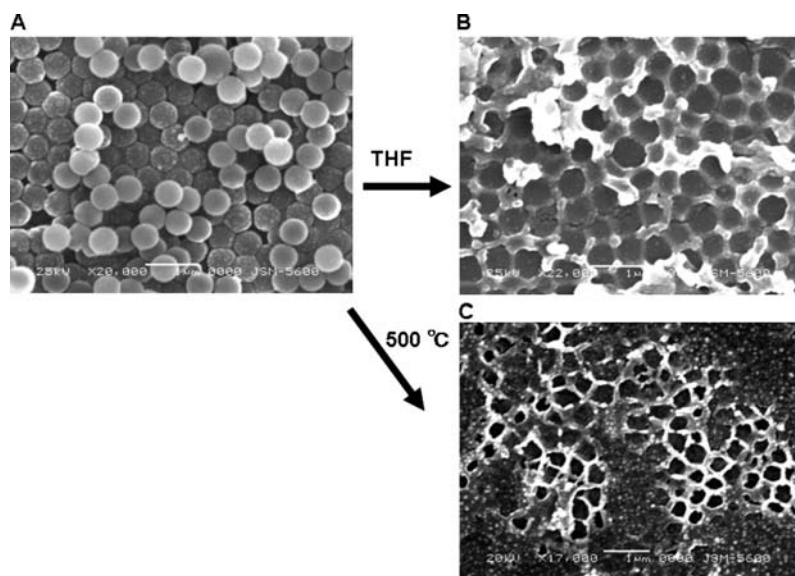


**Fig. 1.12.** SEM images for the nanocomposites by precipitation (a) before (bar:  $5\mu\text{m}$ ) and (b) after the removal of PS templates by heating (bar:  $10\mu\text{m}$ ) and solvent extraction by THF (bar:  $1\mu\text{m}$ )

single type of nanoparticle into self-assembled nanostructures can provide an opportunity to utilize unique properties of the different types of the nanoparticles. The range of properties can be greatly enhanced by organizing two kinds of metal nanoparticles to generate intermetallic nanocomposites due to synergistic effects [158]. Even a physical mixture of two types of metal nanoparticles shows higher catalytic activity than the corresponding monometallic nanoparticles [124, 159–161]. This also proved that combining nanoparticles of different materials allows the manufacture of novel nanocomposite materials. Stable nanostructures, originating from spontaneous self-organization of two kinds of nanoparticles to form nanocomposites, have recently attracted some interest [162–166]. By combining gold nanoparticles stabilized by a carboxylic acid and silica nanoparticles functionalized by a primary amine, acid–base chemistry followed by immediate charge pairing generates electrostatically bound mixed-colloid constructs [162]. Directed self-assembly of two kinds of nanoparticles was performed on a block copolymer micellar template by first introducing Au nanoparticles physically around hexagonally ordered micelles, and then synthesizing chemically  $\text{Fe}_2\text{O}_3$  nanoparticles in the core area of the ordered micelles, resulting in  $\text{Fe}_2\text{O}_3$  nanoparticles surrounded by the Au nanoparticles [163]. Self-organization of Au and CdS nanoparticles by electrostatic interaction led to complex-like structures [164]. Few investigations on self-assembly of two types of metal nanoparticles have been reported except that indirect self-assembly of Au and Ag nanoparticles into bimetallic 3D networks using recognition properties of surface-attached antibodies with bivalent antigens of appropriate double-headed functionalities [165], and evaporation of a mixed colloidal solution of thiol-functionalized Au and Ag nanoparticles on a flat substrate led to self-organization into ordered colloidal superlattices [166]. However, both of them were manipulated on rather limited spatial scales.

When the spherical aggregates of Pd nanoparticles with a mean diameter of 80 nm ( $\text{Pd-NH}_3^+$ ), which were produced by stirring palladium(II) acetate with OAPOSS in methanol at room temperature via self-organized spherical templates of palladium ions and OAPOSS that are involved in electrostatic interaction with  $\text{Au-COO}^-$  as a counterpart building block when spontaneous formation of microporous nanostructures may occur (Fig. 1.13). Microporous nanocomposites of palladium and gold nanoparticles were generated by utilizing electrostatic interaction between oppositely charged gold nanoparticles coated with carboxylate groups ( $\text{Au-COO}^-$ ) and spherical aggregates of palladium nanoparticles ( $\text{Pd-NH}_3^+$ ) with a mean diameter of  $80 \pm 20$  nm stabilized and crosslinked by OAPOSS. Amide bonds were formed between the reactive ion couples well defined in the Pd–Au colloidal nanocomposites during a subsequent chemical reaction to generate more stable nanocomposites with improved chemical and physical properties. Such nanostructures are expected to exhibit excellent catalytic properties for their great surface and synergistic effects of the palladium and gold nanoparticles. Furthermore, amide bonds were formed between the reactive ion couples well defined in the Pd–Au



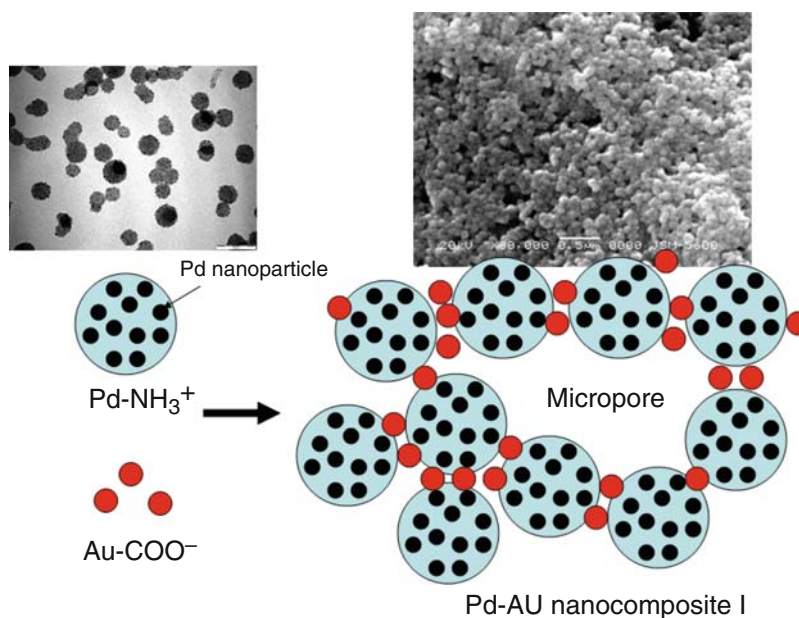


**Fig. 1.13.** Microporous nanocomposite of Pd and Au nanoparticles via electrostatic interaction between Pd-NH<sub>3</sub><sup>+</sup> and Au-COO<sup>-</sup>. TEM image of Pd-NH<sub>3</sub><sup>+</sup> (scale bar: 100 nm) and electron micrographs of Pd-Au nanocomposite I by SEM (bar: 0.5 μm)

colloidal nanocomposites during a subsequent chemical reaction to generate more stable nanocomposites with improved chemical and physical properties as similar as Fig. 1.10. In this system, OAPOSS acts as a primary crosslinker for the palladium nanoparticles to construct Pd-NH<sub>3</sub><sup>+</sup>, and Au-COO<sup>-</sup> was used as a secondary crosslinker for Pd-NH<sub>3</sub><sup>+</sup>.

## 1.5 Organic–Metal 1D Nanostructures

One-dimensional (1D) nanostructures have attracted much attention due to their optical and electronic properties for potential uses as interconnects or active components in fabricating nanodevices [167]. Various chemical methods have been established to accomplish 1D growth of nanostructures [168], among which template-directed synthesis is the most widely used method for generating metallic or metal oxide nanowires [169]. Organic conducting 1D nanostructures have been studied with the expectation for potential application owing to their low density and flexibility for molecular design compared with the inorganic nanostructures [170–173]. Despite a variety of synthetic methods to the organic 1D nanostructures, creation of template-free and facile approaches are still required for future practical application [174, 175].

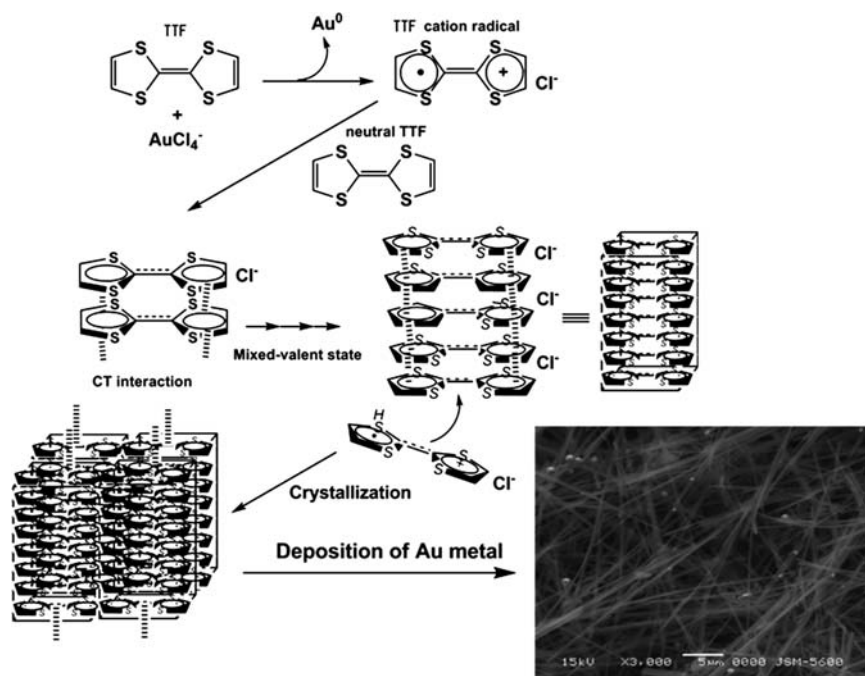


**Fig. 1.14.** Synthesis of organic-metal hybrid nanowires via electron-transfer reaction between TTF and a gold ion and a SEM image of the hybrid nanowires isolated as precipitates from the acetonitrile solution of TTF and  $\text{HAuCl}_4$  after 24 h

Naka and Chujo [176] introduced the synthesis of organic-metal hybrid nanowires via electron-transfer reaction between tetrathiafulvalene (TTF) and a gold ion. The reduction of gold ions by TTF as a reducing reagent is a key process for the formation of the hybrid nanowires as illustrated in Fig. 1.14. An electron-transfer reaction from TTF to gold ions led to the formation of TTF radical cation and zero valent gold ( $\text{Au}^0$ ) [177,178]. Since no gold precipitates were observed, TTF might stabilize gold clusters consisting of  $\text{Au}^0$  at its S sites in the solution. This might act as seeds for the subsequent crystallization of TTF [179]. The 1D crystallization of the intermediate would proceed through the interaction between the neutral and oxidized TTF along the stacking axis of the crystals with chloride anions to form nanocrystallites of TTF chloride. Adsorption and subsequent self-assembly of the resulting gold clusters on lateral dimension of the TTF nanocrystals kinetically controlled 1D crystal growth of TTF, during which the gold clusters acted as a capping agent to inhibit the lateral growth of the TTF nanocrystals by bonding gold surfaces at its S sites (Au-S bonds). The hybrid nanowires as shown in Fig. 1.14 were constructed by cooperative self-organization of the metal and TTF. To our knowledge, this is the first example for creating metal-containing TTF-based hybrid nanowires. The hybrid nanowires are expected to have unique



chemical and physical properties, due to hybridization of metals and organic  $\pi$ -conjugated molecules.

## 1.6 Flocculation of Metal Nanoparticles by Stimuli

Of particular interest is the possibility of tailoring the metal nanoparticles surface with a molecular arrangement consisting of organic molecules that possess responsive properties to certain stimulation. Attempts at controlling the aggregation process have centered on carboxylate-functionalized colloids, which display flocculation behavior as a function of pH [180–182] or cationic species such as metal ions [4, 183]. The ability to functionalize gold nanoparticles with stimuli-responsive property has opened new avenues to utilize these nanomaterials in optical and electronic applications.

Efficient methodologies for responsive self-organization of the metal nanoparticles involve selective control of noncovalent interactions. Several approaches such as hydrogen bonding [180–182],  $\pi$ - $\pi$  interaction [184], host-guest interaction [7, 185], van der Waals forces [186], electrostatic forces [187], antibody-antigen recognition [188], and charge-transfer interaction [189, 190] have been described for the flocculation of the metal nanoparticles (Fig. 1.15). In the following section, several new concepts for the responsive flocculation of metal nanoparticles are described.

### 1.6.1 Photoresponsive Aggregation

Photoactive metal nanoparticles are important for designing light-energy-harvesting devices of nanometric dimension and photocatalysts [191–195]. For examples, Fox and coworkers [193] have demonstrated the ability of gold nanoparticles to preserve the photoreactivity of the *trans*-stilbene and *o*-nitrobenzyl ether moieties similar to the one observed in solution phase. Apart from these studies of discrete nanoparticles, it is also very important to design the photoresponsive aggregation system of metal nanoparticles. Irradiation of UV light to a solution of the gold nanoparticles modified with thymine units resulted in the formation of aggregates comprising chemical crosslinking gold nanoparticles through the photodimerization of the thymine units (Fig. 1.15) [196]. It is well known that thymine bases photodimerize upon the irradiation above 270 nm and revert back to be thymine again upon the irradiation below 270 nm [197–200].

The gold nanoparticles modified with the thymine units were prepared by the same protocol of Brust's method. A water-chloroform two-phase system was used instead of the water-toluene system. The mixture of  $\omega$ -functionalized alkanethiol with the thymine unit and dodecanethiol was added to the chloroform phase to suppress intramolecular photoreaction of the thymine units on the nanoparticle surface. Photoirradiation on the solution of the

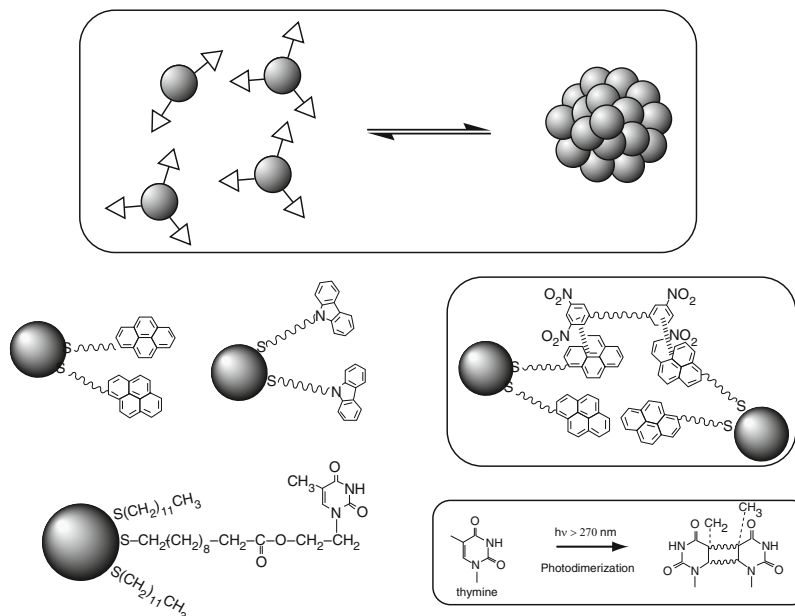


**Fig. 1.15.** Flocculation of metal nanoparticles by stimuli and examples. Thermally reversible self-assembly of metal nanoparticles modified with pyrenyl units or carbazolyl units with the bivalent *m*-dinitrophenyl linker by charge-transfer interaction (*middle*), and photochemical assembly of gold nanoparticles by photodimerization of the thymine units (*lower*)

thymine-functionalized gold nanoparticles was carried out to induce the photodimerization of the thymine. The solution color gradually changed from red to purple with an increase in the reaction time. The surface plasmon band changed from 496 nm to 525, 538, and 544 nm after the photoirradiation for 22, 32, and 46 h, respectively. The precipitation of black powders was observed after 72 h, indicating that the nanoparticle aggregates eventually became too large to remain in the solution. TEM images after the photoirradiation to the solution containing the gold nanoparticles showed the formation of aggregates. The formation of the aggregates with an average diameter of 0.15, 0.25, and 1  $\mu\text{m}$  was observed after 6, 22, and 72 h, respectively. Thus, the degree of colloidal association would be controlled by adjusting photoirradiation time. Aggregation rate was also controlled by turning the thymine unit density on the nanoparticle surface.

### 1.6.2 Metal Nanoparticles Modified with an Ionic Liquid Moiety

The aggregation-induced color changes of the gold nanoparticles in aqueous solutions were demonstrated by using gold nanoparticles modified with an ionic liquid moiety based on imidazolium cation (Fig. 1.16) [201]. The key

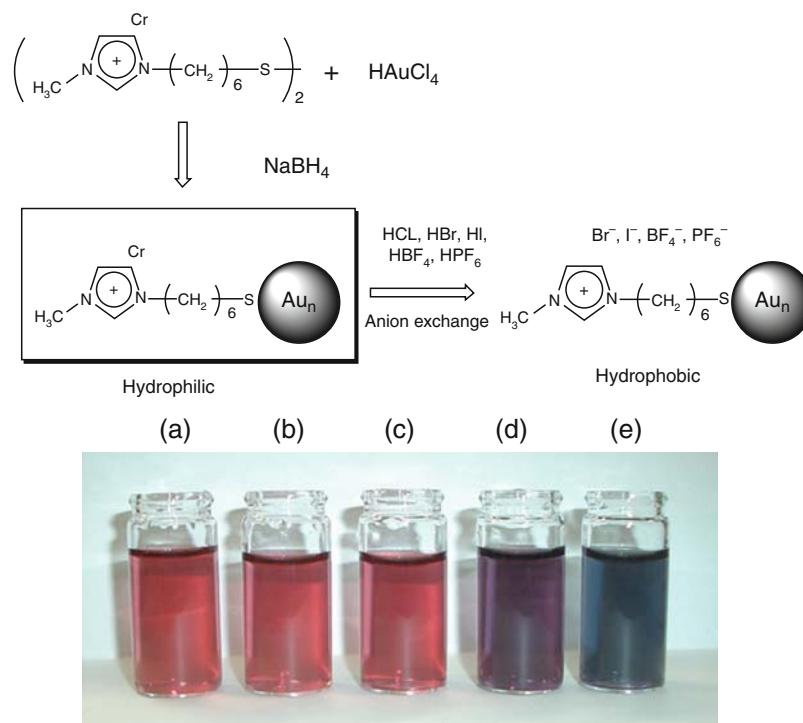


**Fig. 1.16.** Preparation of gold nanoparticle modified with ionic liquid based on the imidazolium cation and their anion exchange

concept of this system is an anion exchange of the imidazolium moiety to control the solubility in solutions. Hydrophilic and hydrophobic properties are tuned by anion exchange of the ionic liquid moiety. Use of the aggregation-induced color changes of the gold nanoparticles in aqueous solutions provides an optical sensor for anions via anion exchange of the ionic liquid moiety. It is well known that the addition of HX ( $\text{X} = \text{BF}_4^-, \text{PF}_6^-$ , and so on) to ionic liquids based on methylimidazolium chloride results in the anion exchange from  $\text{Cl}^-$  to  $\text{BF}_4^-$  or  $\text{PF}_6^-$ , respectively [202, 203]. The reaction of the imidazolium cation-modified gold nanoparticles with various anions was followed as a function of time through optical changes in the surface plasmon resonance in an UV-vis absorption spectrum. In the case of HI and  $\text{HPF}_6$ , the solution color changed dramatically from red to purple and blue, respectively. A TEM image of the obtained solution after addition of HI and  $\text{HPF}_6$  clearly indicated particles aggregates. Elemental analysis of the modified gold nanoparticles after the addition of  $\text{HPF}_6$  showed that 30% of the imidazolium cation immobilized on the nanoparticle surface changed from  $\text{Cl}^-$  to  $\text{PF}_6^-$  by the anion exchange. That is, the surface property of the gold nanoparticles changed from hydrophilic to hydrophobic by the anion exchange of the ionic liquid,

which lead to the nanoparticle aggregation in water. In fact, the imidazolium cation containing  $\text{Cl}^-$  is soluble in water. On the other hand, the imidazolium cation containing  $\text{PF}_6^-$  is immiscible with water. The strength of hydrogen bonding between water molecules and anions in ionic liquids increases in the order of  $\text{PF}_6^- < \text{I}^- < \text{Cl}^-$  [204,205]. Based on the TEM and elemental analysis results, the spectral changes were dominantly induced by the anion exchange under the present conditions, demonstrating that this system can be applied for optical anion sensing.

A new type of gold nanoparticle with a zwitterionic liquid function was prepared using an imidazolium sulfonate-terminated thiol as a capping agent [206]. The zwitterionic liquid is composed of covalently tethered cations and anions, in which the ions do not migrate along a potential gradient. Contrary to the anion-responsive behavior of the gold nanoparticle with the imidazolium cation described above [201], the gold nanoparticle with the zwitterionic liquid were remarkably stable in high concentration of aqueous electrolyte. Lee and coworkers [207] reported that thiol-functionalized imidazolium ionic liquids acted as a highly effective medium for the preparation and stabilization of gold and platinum nanoparticles under a water-phase synthesis. The particle size and uniformity depended on the number of thiol groups and their positions in the thiol-functionalized imidazolium ionic liquids.

Room-temperature ionic liquids are attracting much interest in many fields of chemistry and industry, due to their potential as a “green” recyclable alternative to the traditional organic solvents [208,209]. They are nonvolatile and provide an ultimate polar environment for chemical synthesis. Among various known ionic liquids, ionic liquids containing imidazolium cation and  $\text{PF}_6^-$  has a particularly useful set of properties, being virtually insoluble in water [204,205]. Such biphasic ionic liquid systems have been used to enable simple extraction of products. The modified gold nanoparticles with the imidazolium cations in aqueous phase were transferred across a phase boundary (water to ionic liquid) via the anion exchange of the ionic liquid moiety by addition of  $\text{HPF}_6$  [201]. When  $\text{HPF}_6$  was added to the aqueous solution containing the modified gold nanoparticles with stirring, the ionic liquid phase (1-methyl-3-hexylimidazolium hexafluorophosphate) quickly became colored, drawing from the original deep red color of the aqueous nanoparticles solution. The complete phase transfer of the gold nanoparticles was achieved.

Phase transfer of metal nanoparticles from an aqueous phase to an ionic liquid phase was also reported by Wei and coworkers [210], which does not require the use of a thiol, for the phase transfer of the gold nanoparticles from an aqueous medium to an ionic liquid. An aqueous solution of the gold nanoparticles formed upon the reduction of a solution of  $\text{HAuCl}_4$  with citrate was added to the organic phase. The water-immiscible ionic liquid, 1-butyl-3-methylimidazolium hexafluorophosphate is a solvent medium that allows complete transfer of the gold nanoparticles from an aqueous phase into an organic phase. Water-soluble cationic CdTe nanocrystals, which were prepared by an aqueous synthetic approach, were efficiently extracted from an aqueous

phase into a water-immiscible ionic liquid [211]. The ionic liquid containing the transferred metal nanoparticles has potential for the recyclable biphasic catalysis process.

pH-Responsive system in aqueous solution has extremely promising prospect. Many biological phenomena, e.g., cellular recognition and transportation in tissues and organs, are largely concerned to pH at which they occur. There have been several reports for pH-responsive metal nanoparticles [182,212–215]. Toshima and coworkers synthesized 3-mercaptopropionic acid-modified gold nanoparticles and reversibly controlled the colloidal dispersions by using interparticle hydrogen bonds or electrostatic repulsion depending on pH. Lee and coworkers [214] synthesized gold nanoparticles coated by a hydrogel consisting of poly(acrylic acid-*co*-*N*-isopropylacrylamide) and acted as an interrupter of surface plasmon absorbance depending on pH and temperature.

Naka and Chujo [216] reported pH-responsive control of the colloidal dispersions of the imidazolium cation-modified gold nanoparticles using a combination of poly(acrylic acid) (PAA) in aqueous solution. The strategy is based on the electrostatic interaction between the imidazolium cations on the surface of the gold nanoparticles and the carboxylate anions of PAA. The resulting precipitate after the imidazolium cation-modified gold nanoparticles was mixed with PAA (MW = 25,000) in aqueous solution, as described above, was dissolved into a clear red colored solution when the pH dropped below 1.9 by the addition of 1.0 M HCl. Addition of 1.0 M NaOH to the acidified solution caused a precipitate again at the pH of 2.2, and the precipitate was redissolved when the pH rose above 5.5 (Fig. 1.17). Addition of 1.0 M HCl to the final solution reproduced the precipitation–redispersion process until the pH dropped below 1.9. The absorption maximum of the solution at pH 6.0 was redshifted compared with that in the case of the solution at pH 1.7 and the pristine solution of the imidazolium cation-modified gold nanoparticles without PAA ( $\lambda_{\text{max}} = 514 \text{ nm}$ ). The redshift can be attributed to the coupled plasmon absorbance of the gold nanoparticles in closer contact, which indicates a formation of particle aggregates in the aqueous solution at pH 6.0. The TEM image of the sample at pH 6.0 shows the aggregates of the gold nanoparticles and the size of the aggregates was ranging from 40 to 150 nm. A DLS measurement suggested the formation of the aggregates in aqueous solution with a diameter of  $115 \pm 21 \text{ nm}$ .

There are several reports about the phenomena of nanoparticles-based flocculation by charged polymers [217–223]. Although extensive experimental and theoretical works are reported for understanding the flocculation processes and construct nanoparticles-based flocculated materials with controlled structures, studies for pH-responsive phenomena of nanoparticles-based flocculated materials were limited. Sehgal et al. [223] reported a precipitation–redispersion mechanism for complexation of short chain PAA with cerium oxide nanoparticles. They showed that addition of PAA to a cerium oxide solutions leads to macroscopic precipitation and the solution redispersed into a clear sols of single particles with an anionic PAA corona as the pH increased.

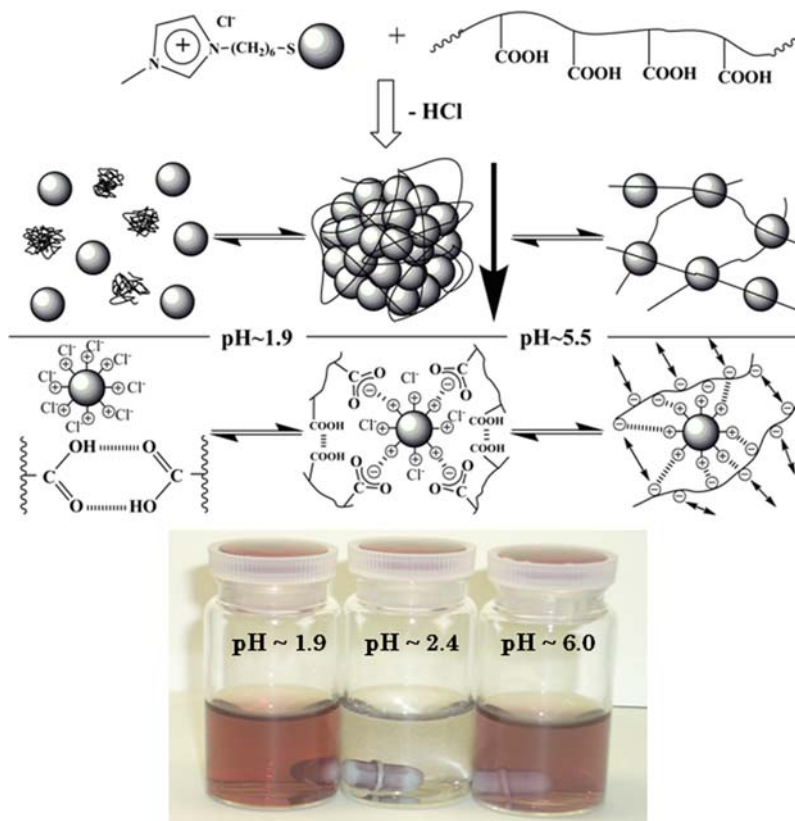


**Fig. 1.17.** Photograph of various pH solutions of the imidazolium cation-modified gold nanoparticles with PAA (MW = 25,000) and proposed mechanism of the flocculation and the pH-responsive aggregation of the imidazolium cation-modified gold nanoparticles with PAA

We found a different precipitation–redispersion behavior for the complexes of the imidazolium cations-modified gold nanoparticles with PAA [216].

## 1.7 Conclusion and Outlook

Metal nanoparticles can be functionalized with a wide variety of structural units using simple chemical process under moderate condition. Stabilization of metal nanoparticles by ligand units such as thiols or amines enable further manipulation of usual compounds. Since close-packed assembly of metal nanoparticles is expected to produce different electronic, magnetic, and optical functions based on quantum mechanical coupling of conduction electron localized in each metal nanoparticles, development of simple and easy methods

for the organization of metal nanoparticles is indispensable for preparing new nanodevices.

To exploit metal nanoparticle properties for future device fabrication, self-organization of nanoparticles in controlled manner is required from the standpoint of the “bottom-up” approach. Dendritic molecules mediate assembly of the metal nanoparticles shows potential for controlling into one-, two-, and three-dimensional structures. It is well established that dendrimers have acted as excellent hosts for the formation and stabilization of metal nanoparticles. However, research direction of using dendrimers as linkers for metal nanoparticles is limited. Since dendrimers are monodisperse macromolecules prepared by completely designed chemical synthesis, combination of the metal nanoparticle-based building blocks and the dendrimers would provide a variety of nanocomposites in controlled self-organization. Only one disadvantage of using dendrimers is their multistep chemical synthesis. Polyhedral oligosilsesquioxanes, however, should be excellent candidates for this purpose due to their easy preparation.

Particular interest is focused on the functionalized metal nanoparticles that possess responsive properties to certain stimulation such as pH, anion, cation, temperature, light, small molecules, and biological molecules. Methodologies for responsive self-organization usually involve using noncovalent interaction, such as electrostatic interaction, hydrogen bonding,  $\pi$ - $\pi$  interaction, charge-transfer interaction, and host-guest interaction. Using reversible chemical bond formation is also available. Changing solubility, such as hydrophobic and hydrophilic properties, of metal nanoparticles is an alternative way to self-assemble especially in aqueous solution. Use of the aggregation-induced color changes of gold nanoparticles provides these responsive colloidal solutions as an optical sensor for guest ions and molecules.

Key and basic requirements for future development in this field include further seeking and optimization of controlled synthesis of the nanoparticle-based building blocks. Although lowering size distribution of the nanoparticles with controlled diameter should be a central target, design and synthesis of functional materials with simple coating needs contribution of organic and polymer synthetic chemists. We expect that the continuous cooperation of organic and polymer chemists with inorganic and physical chemists, which is desirable to fabricate the metal nanoparticles-based hybrid materials, will lead to the next industrial revolution.

## References

1. A.C. Templeton, W.P. Wuelfing, R.W. Murray, *Acc. Chem. Res.* **33**, 27 (2000)
2. M.-C. Daniel, D. Astruc, *Chem. Rev.* **104**, 293 (2004)
3. S.O. Obare, R.E. Holowell, C.J. Murphy, *Langmuir* **18**, 10407 (2002)
4. Y. Kim, R.C. Johnson, J.T. Hupp, *Nano Lett.* **1**, 165 (2001)
5. S. Watanabe, M. Sonobe, M. Arai, Y. Tazume, T. Matsuo, T. Nakamura, K. Yoshida, *Chem. Commun.* 2866 (2002)



6. C.A. Mirkin, R.L. Letsinger, R.C. Mucic, J.J. Storhoff, *Nature* **382**, 607 (1996)
7. S.Y. Lin, S.W. Liu, C.M. Lin, C.H. Chen, *Anal. Chem.* **74**, 330 (2002)
8. G. Chumanov, K. Sokolov, B.W. Gregory, T.M. Cotton, *J. Phys. Chem.* **99**, 9466 (1995)
9. S. Nie, S.R. Emory, *Science* **275**, 1102 (1997)
10. J.A. Dahl, B.L.S. Maddux, J.E. Hutchison, *Chem. Rev.* **107**, 2228 (2007)
11. H. Hirai, Y. Nakao, N. Toshima, K. Adachi, *Chem. Lett.* 905 (1976)
12. H. Hirai, Y. Nakao, N. Toshima, *J. Macromol. Sci. Chem. A* **12**, 1117 (1978)
13. R.P. Andres, J.D. Bielefeld, J.I. Henderson, D.B. Janes, V.R. Kolagunta, C.P. Kubiak, W.J. Mahoney, R.G. Osifchin, *Science* **273**, 1690 (1996)
14. C.P. Collier, R.J. Saykally, J.J. Shiang, S.E. Henrichs, J.R. Heath, *Science* **277**, 1978 (1997)
15. M. Brust, M. Walker, D. Bethell, D.J. Schiffrin, R. Whyman, *J. Chem. Soc., Chem. Commun.* 801 (1994)
16. M.J. Hostetler, C.-J. Zhong, B.K.H. Yen, J. Anderegg, S.M. Gross, N.D. Evans, M. Porter, R.W. Murray, *J. Am. Chem. Soc.* **120**, 922 (1998)
17. A.C. Templeton, M.J. Hostetler, C.T. Kraft, R.W. Murray, *J. Am. Chem. Soc.* **120**, 1906 (1998)
18. M.J. Hostetler, A.C. Templeton, R.W. Murray, *Langmuir* **15**, 3782 (1999)
19. A.C. Templeton, S. Chen, S.M. Gross, R.W. Murray, *Langmuir* **15**, 66 (1999)
20. T. Yonezawa, T. Kunitake, *Colloids Surf. A, Physicochem. Eng. Asp.* **149**, 193 (1999)
21. D.V. Leff, L. Brandt, J.R. Heath, *Langmuir* **12**, 4723 (1996)
22. N.R. Jana, X. Peng, *J. Am. Chem. Soc.* **125**, 14280 (2003)
23. H. Hiramatsu, F.E. Osterloh, *Chem. Mater.* **16**, 2509 (2004)
24. M. Aslam, L. Fu, M. Su, K. Vijayamohanan, V.P. David, *J. Mater. Chem.* **14**, 1795 (2004)
25. G. Schmid, V. Maihack, F. Lantermann, S. Peschel, *J. Chem. Soc., Dalton Trans.* 589 (1996)
26. M.N. Vargaftik, V.P. Zagorodnikov, I.P. Stolyarov, I.I. Moiseev, V.A. Likholobov, D.I. Kochubey, A.L. Chuvilin, V.I. Zaikovskiy, K.I. Zamaraev, G.I. Timofeeva, *J. Chem. Soc., Chem. Commun.* 937 (1985)
27. G. Schmid, M. Harms, J. Malm, J. Bovin, J. Ruitenbeck, H.W. Zandbergen, W.T. Fu, *J. Am. Chem. Soc.* **115**, 2046 (1993)
28. G. Schmid, B. Morum, J. Malm, *Angew. Chem. Int. Ed. Engl.* **28**, 778 (1989)
29. A. Duteil, G. Schmid, W. Meyer-Zaika, *J. Chem. Soc., Chem. Commun.* 31 (1995)
30. G. Schmid, R. Pfeil, R. Boese, F. Bandermann, S. Meyer, G.H.M. Calis, J.W.A. Van der Velden, *Chem. Ber.* **114**, 3634 (1981)
31. W.W. Weare, S.M. Reed, M.G. Warner, J.E. Hutchison, *J. Am. Chem. Soc.* **122**, 12890 (2000)
32. J. Petroski, M.H. Chou, C. Creutz, *Inorg. Chem.* **43**, 1597 (2004)
33. G.H. Woehrle, L.O. Brown, J.E. Hutchison, *J. Am. Chem. Soc.* **127**, 2172 (2005)
34. R. Balasubramanian, R. Guo, A.J. Mills, R.W. Murray, *J. Am. Chem. Soc.* **127**, 8126 (2005)
35. Y. Shichibu, Y. Negishi, T. Tsukuda, T. Teranishi, *J. Am. Chem. Soc.* **127**, 13464 (2005)
36. J.G. Worden, A.W. Shaffer, Q. Huo, *Chem. Commun.* 518 (2004)



37. K.-M. Sung, D.W. Mosley, B.R. Peelle, S. Zhang, J.M. Jacobson, *J. Am. Chem. Soc.* **126**, 5064 (2004)
38. R. Sardar, T.B. Heap, J.S. Shumaker-Parry, *J. Am. Chem. Soc.* **129**, 5356 (2007)
39. Q. Dai, J.G. Worden, J. Trullinger, Q. Huo, *J. Am. Chem. Soc.* **127**, 8008 (2005)
40. G. Ramakrishna, Q. Dai, J. Zou, Q. Huo, T. Goodson III, *J. Am. Chem. Soc.* **129**, 1848 (2007)
41. A.M. Jackson, J.W. Myerson, F. Stellacci, *Nat. Mater.* **18**, 330 (2004)
42. A.M. Jackson, Y. Hu, P.J. Silva, F. Stellacci, *J. Am. Chem. Soc.* **128**, 11135 (2006)
43. G.A. DeVries, M. Brunnbauer, Y. Hu, A.M. Jackson, B. Long, B.T. Neltner, O. Uzun, B.H. Wunsch, F. Stellacci, *Science* **315**, 358 (2007)
44. K. Naka, M. Yaguchi, Y. Chujo, *Chem. Mater.* **11**, 849 (1999)
45. A.B.R. Mayer, J.E. Mark, *PMSE Preprints* **73**, 220 (1995)
46. W.P. Wuelfing, S.M. Gross, D.T. Miles, R.W. Murray, *J. Am. Chem. Soc.* **120**, 12696 (1998)
47. J. Shan, M. Nuopponen, H. Jiang, E. Kauppinen, H. Tenhu, *Macromolecules* **36**, 4526 (2003)
48. C. Mangeney, F. Ferrage, I. Aujard, V. Marchi-Artzner, L. Jullien, O. Ouari, E.D. Rekaï, A. Laschewsky, I. Vikholm, J.W. Sadowski, *J. Am. Chem. Soc.* **124**, 5811 (2002)
49. M.K. Corbierre, N.S. Cameron, M. Sutton, S.G.J. Mochrie, L.B. Lurio, A. Rhm, R.B. Lennox, *J. Am. Chem. Soc.* **123**, 10411 (2001)
50. J.J. Chiu, B.J. Kim, E.J. Kramer, D.J. Pine, *J. Am. Chem. Soc.* **127**, 5036 (2005)
51. E.R. Zubarev, J. Xu, A. Sayyad, J.D. Gibson, *J. Am. Chem. Soc.* **128**, 4958 (2006)
52. K. Ohno, K. Koh, Y. Tsujii, T. Fukuda, *Macromolecules* **35**, 8989 (2002)
53. T.K. Mandal, M.S. Fleming, D.R. Walt, *Nano Lett.* **2**, 3 (2002)
54. J. Raula, J. Shan, M. Nuopponen, A. Niskanen, H. Jiang, E.I. Kauppinen, H. Tenhu, *Langmuir* **19**, 3499 (2003)
55. D. Rutot-Houze, W. Fris, P. Degee, P. Dubois, *J. Macromol. Sci. Pure Appl. Chem. A* **41**, 697 (2004)
56. H. Itoh, K. Naka, Y. Chujo, *Polym. Bull.* **46**, 357 (2001)
57. R. Gangopadhyay, A. De, *Chem. Mater.* **12**, 608 (2000)
58. K.G. Neoh, T.T. Young, N.T. Looi, E.T. Kang, K.L. Tan, *Chem. Mater.* **9**, 2906 (1997)
59. K.V. Sarathy, K.S. Narayan, J. Kim, J.O. White, *Chem. Phys. Lett.* **318**, 543 (2000)
60. T. Hertel, E. Knoesel, M. Wolf, G. Ertl, *Phys. Rev. Lett.* **76**, 535 (1996)
61. F. Ficicoglu, F. Kadirgan, *J. Electroanal. Chem.* **451**, 95 (1998)
62. C.S.C. Bose, K. Rajeshwar, *J. Electroanal. Chem.* **333**, 235 (1992)
63. S.W. Huang, K.G. Neoh, C.W. Shih, D.S. Lim, E.T. Kang, H.S. Han, K.L. Tan, *Synth. Met.* **96**, 117 (1998)
64. K.G. Neoh, K.K. Tan, P.L. Goh, S.W. Huang, E.T. Kang, K.L. Tan, *Polymer* **40**, 887 (1999)
65. S.W. Huang, K.G. Neoh, E.T. Kang, H.S. Han, K.L. Tan, *J. Mater. Chem.* **8**, 1743 (1998)

66. Y. Zhou, H. Itoh, T. Uemura, K. Naka, Y. Chujo, *Chem. Commun.* 613 (2001)
67. Y. Zhou, H. Itoh, T. Uemura, K. Naka, Y. Chujo, *Langmuir* **18**, 277 (2002)
68. K. Naka, T. Uemura, Y. Chujo, *Macromolecules* **32**, 4641 (1999)
69. M.A. Hempenius, B.M.W. Langeveld-Voss, J.A.E.H. van Haare, R.A.J. Janssen, S.S. Sheiko, J.P. Spatz, M. Möller, E.W. Meijer, *J. Am. Chem. Soc.* **120**, 2798 (1998)
70. J.H. Youk, J. Locklin, C. Xia, M.-K. Park, R. Advincula, *Langmuir* **17**, 4681 (2001)
71. T. Sanji, Y. Ogawa, Y. Nakatsuka, M. Tanaka, H. Sakurai, *Chem. Lett.* **32**, 980 (2003)
72. G. Schmid, M. Bämle, M. Geerkens, I. Heim, C. Osemann, T. Sawitowski, *Chem. Soc. Rev.* **28**, 179 (1999)
73. C.N.R. Rao, G.U. Kulkarni, P. John Thomas, P.P. Edwards, *Chem. Soc. Rev.* **29**, 27 (2000)
74. G. Schmid, L.F. Chi, *Adv. Mater.* **10**, 515 (1998)
75. Y. Xia, J.A. Rogers, K.E. Paul, G.M. Whitesides, *Chem. Rev.* **99**, 1823 (1999)
76. R. Elghanian, J.J. Storhoff, R.C. Mucic, R.L. Letsinger, C.A. Mirkin, *Science* **277**, 1078 (1997)
77. C. Stowell, B.A. Korgel, *Nano Lett.* **1**, 595 (2001)
78. P.C. Ohara, W.M. Gelbart, *Langmuir* **14**, 3418 (1998)
79. M. Sastry, M. Rao, K.N. Ganesh, *Acc. Chem. Res.* **35**, 847 (2002)
80. A.K. Boal, F. Llhana, J.E. Derouchey, T. Thurn-Albrecht, T.P. Russell, V.M. Rotello, *Nature* **404**, 746 (2000)
81. A.K. Boal, V.M. Rotello, *J. Am. Chem. Soc.* **122**, 734 (2000)
82. J.J. Storhoff, A.A. Lazarides, R.C. Mucic, C.A. Mirkin, R.L. Letsinger, G.C. Schatz, *J. Am. Chem. Soc.* **122**, 4640 (2000)
83. M. Brust, D. Bethell, D.J. Schiffrin, C.J. Kiely, *Adv. Mater.* **7**, 795 (1995)
84. R. Shenhar, T.B. Norsten, V.M. Rotello, *Adv. Mater.* **17**, 657 (2005)
85. M. Antonietti, C. Göltner, *Angew. Chem. Int. Ed. Engl.* **36**, 910 (1997)
86. M.D. Musick, C.D. Keating, M.H. Keefen, M.J. Natan, *Chem. Mater.* **9**, 1499 (1997)
87. D. Bethell, M. Brust, D.J. Schiffrin, C. Kiely, *Electroanal. Chem.* **409**, 137 (1996)
88. A. Doron, E. Katz, I. Willner, *Langmuir* **11**, 1313 (1995)
89. R.G. Freeman, K.C. Grabar, K.J. Allison, R.M. Bright, J.A. Davis, A.P. Guthrie, M.B. Hommer, M.A. Jackson, P.C. Smith, D.G. Walter, M.J. Natan, *Science* **267**, 1629 (1995)
90. K.C. Grabar, R.G. Freeman, M.B. Hommer, M.J. Natan, *Anal. Chem.* **67**, 735 (1995)
91. J.R. Heath, C.M. Knobler, D.V. Leff, *J. Phys. Chem. B* **101**, 189 (1997)
92. B.O. Dabbousi, C.B. Murray, M.F. Rubner, M.G. Bawendi, *Chem. Mater.* **6**, 216 (1994)
93. M. Giersig, P. Mulvaney, *Langmuir* **9**, 3408 (1993)
94. T. Teranishi, M. Hosoe, M. Miyake, *Adv. Mater.* **9**, 65 (1997)
95. J. Schmitt, G. Decher, W.J. Dressick, S.L. Brandow, R.E. Geer, R. Shashidhar, J.M. Calvert, *Adv. Mater.* **9**, 61 (1997)
96. N.A. Kotov, I. Dékány, J.H. Fendler, *J. Phys. Chem.* **99**, 13065 (1995)
97. T. Yonezawa, S. Onoue, T. Kunitake, *Chem. Lett.* 1061 (1999)
98. G. Schmid, M. Bäumle, N. Beyer, *Angew. Chem. Int. Ed.* **39**, 181 (2000)

99. G.L. Hornyak, M. Krll, R. Pugin, T. Sawaitowski, G. Schmid, J.-O. Bovin, G. Karsson, H. Hofmeister, S. Hopfe, *Chem. Eur. J.* **3**, 1951 (1997)
100. G. Schmid, R. Pugin, J.-O. Malm, J.-O. Bovin, *Eur. J. Inorg. Chem.* **6**, 813 (1998)
101. T. Teranishi, A. Sugawara, T. Shimizu, M. Miyake, *J. Am. Chem. Soc.* **124**, 4210 (2002)
102. T. Oku, K. Suganuma, *Chem. Commun.* 2355 (1999)
103. E. Fort, C. Ricolleau, J. Sau-Pueyo, *Nano Lett.* **3**, 65 (2003)
104. E. Braun, Y. Eichen, U. Sivan, G. Ben-Yoseph, *Nature* **391**, 775 (1998)
105. J. Richter, R. Seidel, R. Krisch, M. Mertig, W. Pompe, J. Plaschke, H.K. Schackert, *Adv. Mater.* **12**, 507 (2000)
106. W.E. Ford, O. Harnack, A. Yasuda, J.M. Wessels, *Adv. Mater.* **13**, 1793 (2001)
107. M. Mertig, L. Colombi Ciacchi, R. Seidel, W. Pompe, A. De Vita, *Nano Lett.* **2**, 841 (2002)
108. O. Harnack, W.E. Ford, A. Yasuda, J.M. Wessels, *Nano Lett.* **2**, 919 (2002)
109. A. Kumar, M. Pattarkine, M. Bhadbhade, A.B. Mandale, K.N. Ganesh, S.S. Datar, C.V. Dharmadhikari, M. Sastry, *Adv. Mater.* **13**, 341 (2001)
110. M.G. Warner, J.E. Hutchison, *Nat. Mater.* **2**, 272 (2003)
111. C.M. Niemeyer, W. Bürger, J. Peplies, *Angew. Chem. Int. Ed.* **37**, 2265 (1998)
112. R. Djalali, Y.-F. Chen, H. Matsui, *J. Am. Chem. Soc.* **124**, 13660 (2002)
113. C.A. Berven, L. Clarke, J.L. Mooster, M.N. Wybourne, J.E. Hutchison, *Adv. Mater.* **13**, 109 (2001)
114. E. Dujardin, C. Peet, G. Stubbs, J.N. Culver, S. Mann, *Nano Lett.* **3**, 413 (2003)
115. S.L. Burkett, S. Mann, *Chem. Commun.* 321 (1996)
116. S. Fullam, D. Cattel, H. Rensmo, D. Fitzmaurice, *Adv. Mater.* **12**, 1430 (2000)
117. K. Jiang, A. Eitan, L.S. Schadler, P.M. Ajayan, R.W. Siegel, N. Grobert, M. Mayne, M. Reyes-Reyes, H. Terrones, M. Terrones, *Nano Lett.* **3**, 275 (2003)
118. A. Kivity, S. Minko, G. Gorodyska, M. Stamm, W. Jaeger, *Nano Lett.* **2**, 881 (2002)
119. B.W. Maynor, Y. Li, J. Liu, *Langmuir* **17**, 2575 (2001)
120. L.M. Demers, C.A. Mirkin, *Angew. Chem. Int. Ed.* **40**, 3069 (2001)
121. H. Zhang, Z. Li, C.A. Mirkin, *Adv. Mater.* **14**, 1472 (2002)
122. M.F. Ottaviani, S. Bossmann, N.J. Turro, D.A. Tomalia, *J. Am. Chem. Soc.* **116**, 661 (1994)
123. M. Zhao, L. Sun, R.M. Crooks, *J. Am. Chem. Soc.* **120**, 4877 (1998)
124. K. Esumi, A. Suzuki, N. Aihara, K. Usui, K. Torigoe, *Langmuir* **14**, 3157 (1998)
125. K. Esumi, A. Suzuki, A. Yamashita, K. Torigoe, *Langmuir* **16**, 2604 (2000)
126. M.C. Garcia, L.A. Baker, R.M. Crooks, *Anal. Chem.* **71**, 256 (1999)
127. K. Hayakawa, T. Yoshimura, K. Esumi, *Langmuir* **19**, 5517 (2003)
128. R.M. Laine, C. Zhang, A. Sellinger, L. Viculis, *Appl. Organomet. Chem.* **12**, 715 (1998)
129. J. Choi, J. Harcup, A.F. Yee, Q. Zhu, R.M. Laine, *J. Am. Chem. Soc.* **123**, 11420 (2001)
130. K. Naka, M. Fujita, K. Tanaka, Y. Chujo, *Langmuir* **23**, 9057 (2007)
131. F.J. Feher, K.D. Wyndham, *Chem. Commun.* 323 (1998)
132. M.C. Gravel, C. Zhang, M. Dinderman, R.M. Laine, *Appl. Organomet. Chem.* **13**, 329 (1999)
133. H. Itoh, K. Naka, Y. Chujo, *Bull. Chem. Soc. Jpn.* **77**, 1767 (2004)

134. B.L. Frankamp, A.K. Boal, V.M. Rotello, *J. Am. Chem. Soc.* **124**, 15146 (2002)
135. K. Naka, H. Itoh, Y. Chujo, *Nano Lett.* **2**, 1183 (2002)
136. H. Bönemann, G. Braun, W. Brijoux, R. Brinkmann, A.S. Tilling, K. Seevogel, K. Siepen, *J. Organomet. Chem.* **520**, 142 (1996)
137. A.B.R. Mayer, J.E. Mark, R.E. Morris, *Polym. J.* **30**, 197 (1998)
138. H. Tanaka, S. Koizumi, T. Hashimoto, H. Itoh, M. Satoh, K. Naka, Y. Chujo, *Macromolecules* **40**, 4327 (2007)
139. K. Naka, H. Itoh, Y. Chujo, *Chem. Lett.* **33**, 1236 (2004)
140. J.B. Carroll, B.L. Frankamp, V.M. Rotello, *Chem. Commun.* 1892 (2002)
141. J.B. Carroll, B.L. Frankamp, S. Srivastava, V.M. Rotello, *J. Mater. Chem.* **14**, 690 (2004)
142. X. Wang, K. Naka, H. Itoh, Y. Chujo, *Chem. Lett.* **33**, 216 (2004)
143. T. Cassagneau, F. Caruso, *J. Am. Chem. Soc.* **124**, 8172 (2002)
144. D.G. Shchukin, R.A. Caruso, *Chem. Commun.* 1478 (2003)
145. M.D. Musick, C.D. Keating, M.H. Keefe, M.J. Natan, *Chem. Mater.* **9**, 1499 (1997)
146. G. Decher, J.D. Hong, J. Schmitt, *Thin Solid Films* **210/211**, 831 (1992)
147. Y. Lvov, G. Decher, H. Moehwald, *Langmuir* **9**, 481 (1993)
148. D.I. Svergun, M.B. Kozin, P.V. Konarev, E.V. Shtykova, V.V. Volkov, D.M. Chernyshov, P.M. Valetsky, L.M. Bronstein, *Chem. Mater.* **12**, 3552 (2000)
149. J. Zhang, L. Bai, K. Zhang, Z. Cui, G. Zhang, B. Yang, *J. Mater. Chem.* **13**, 514 (2003)
150. M.D. Musick, C.D. Keating, L.A. Lyon, S.L. Botsko, D.J. Peña, W.D. Holliway, T.M. McEvoy, J.N. Richardson, M.J. Natan, *Chem. Mater.* **12**, 2869 (2000)
151. F.P. Zamborini, J.F. Hicks, R.W. Murray, *J. Am. Chem. Soc.* **122**, 4514 (2000)
152. N. Krasteva, I. Besnard, B. Guse, R.E. Bauer, K. Mülen, A. Yasuda, T. Vossmeier, *Nano Lett.* **2**, 551 (2002)
153. X. Wang, K. Naka, M. Zhu, H. Kuroda, H. Itoh, Y. Chujo, *J. Inorg. Organomet. Polym. Mater.* **17**, 447 (2007)
154. D.M. Shchukin, R.A. Caruso, *Chem. Commun.* 1478 (2003)
155. B. Rodríguez-González, V. Salgueiro-Maceira, F. García-Santamaría, L.M. Liz-Marzán, *Nano Lett.* **2**, 471 (2002)
156. Y. Zhou, S.-H. Yu, A. Thomas, B.-H. Han, *Chem. Commun.* 262 (2003)
157. M.S. Wong, J.N. Cha, K.-S. Choi, T.J. Deming, G.D. Stucky, *Nano Lett.* **2**, 583 (2002)
158. S. Darby, T.V. Mortimer-Jones, R.L. Johnston, C. Roberts, *J. Chem. Phys.* **116**, 1536 (2002)
159. N. Toshima, K. Hirakawa, *Appl. Surf. Sci.* **121/122**, 534 (1997)
160. K. Hirakawa, N. Toshima, *Chem. Lett.* **32**, 78 (2003)
161. T. Sehayek, M. Lahav, R. Popovltz-Biro, A. Vaskevich, I. Rubinstein, *Chem. Mater.* **17**, 3743 (2005)
162. T.H. Galow, A.K. Boal, V.M. Rotello, *Adv. Mater.* **12**, 576 (2000)
163. B.-H. Sohn, J.-M. Choi, S.I. Yoo, S.-H. Yun, W.-C. Zin, J.-C. Jung, M. Kanehara, T. Hirata, T. Teranishi, *J. Am. Chem. Soc.* **125**, 6368 (2003)
164. J. Kolny, A. Kornowski, H. Weller, *Nano Lett.* **2**, 361 (2002)
165. W. Shenton, S.A. Davis, S. Mann, *Adv. Mater.* **11**, 449 (1999)
166. C.J. Kiely, J. Fink, J.G. Zheng, M. Brust, D. Bethell, D.J. Schiffrin, *Adv. Mater.* **12**, 640 (2000)
167. M.Y. Han, C.H. Quek, *Langmuir* **16**, 362 (2000)

168. T.S. Ahmadi, Z.L. Wang, A. Henglein, M.A. El-Sayed, *Science* **272**, 1924 (1996)
169. Y. Xia, P. Yang, Y. Sun, B. Mayers, B. Gates, Y. Yin, F. Kim, H. Yan, *Adv. Mater.* **15**, 353 (2003)
170. J. Haung, S. Virji, B.H. Weiller, R.B. Kaner, *J. Am. Chem. Soc.* **125**, 314 (2003)
171. J.-J. Chiu, C.-C. Kei, T.-P. Perng, W.-S. Wang, *Adv. Mater.* **15**, 1361 (2003)
172. H. Liu, Q. Zhao, Y. Li, Y. Liu, F. Lu, J. Zhuang, S. Wang, L. Jiang, D. Zhu, D. Yu, L. Chi, *J. Am. Chem. Soc.* **127**, 1120 (2005)
173. H. Gan, H. Liu, Y. Li, Q. Zhao, Y. Li, S. Wang, T. Jiu, N. Wang, X. He, D. Yu, D. Zhu, *J. Am. Chem. Soc.* **127**, 12452 (2005)
174. T. Akutagawa, T. Ohta, T. Hasegawa, T. Nakamura, C.A. Christensen, *Proc. Natl. Acad. Sci. USA* **99**, 5028 (2002)
175. K. Yasui, N. Kimizuka, *Chem. Lett.* **34**, 248 (2005)
176. K. Naka, D. Ando, X. Wang, Y. Chujo, *Langmuir* **23**, 3450 (2007)
177. X. Wang, H. Itoh, K. Naka, Y. Chujo, *Chem. Commun.* 1300 (2002)
178. X. Wang, H. Itoh, K. Naka, Y. Chujo, *Langmuir* **19**, 6242 (2003)
179. F. Favier, H. Liu, R.M. Penner, *Adv. Mater.* **13**, 1567 (2001)
180. J. Simard, C. Briggs, A.K. Boal, V.M. Rotello, *Chem. Commun.* 1943 (2000)
181. M. Sastry, K.S. Mayya, K. Bandyopadhyay, *Colloids Surf. A* **127**, 221 (1997)
182. Y. Shiraishi, D. Arakawa, N. Toshima, *Eur. Phys. J. E* **8**, 377 (2002)
183. A.N. Shipway, M. Lahav, R. Gabai, I. Willner, *Langmuir* **16**, 8789 (2000)
184. J. Jin, T. Iyoda, C. Cao, Y. Song, L. Jiang, T.J. Li, D.B. Zhu, *Angew. Chem. Int. Ed.* **40**, 2135 (2001)
185. J. Liu, S. Mendoza, E. Roman, M.J. Lynn, R. Xu, A.E. Kaifer, *J. Am. Chem. Soc.* **121**, 4304 (1999)
186. V. Patil, K.S. Mayya, S.D. Pradhan, M. Sastry, *J. Am. Chem. Soc.* **119**, 9281 (1997)
187. F. Caruso, R.A. Caruso, H. Mohwald, *Science* **282**, 1111 (1998)
188. W. Shenton, W.A. Davis, S. Mann, *Adv. Mater.* **11**, 449 (1999)
189. K. Naka, H. Itoh, Y. Chujo, *Langmuir* **19**, 5496 (2003)
190. K. Naka, H. Itoh, Y. Chujo, *Bull. Chem. Soc. Jpn.* **78**, 501 (2005)
191. A. Manna, P.-L. Chen, H. Akiyama, T.-X. Wei, K. Tamada, W. Knoll, *Chem. Mater.* **15**, 20 (2003)
192. B.I. Ipe, S. Mahima, K.G. Thomas, *J. Am. Chem. Soc.* **125**, 7174 (2003)
193. J. Hu, J. Zhang, F. Liu, K. Kittredge, J.K. Whitesell, M.A. Fox, *J. Am. Chem. Soc.* **123**, 1464 (2001)
194. J. Zhang, J.K. Whitesell, M.A. Fox, *Chem. Mater.* **13**, 2323 (2001)
195. P.V. Kamat, *J. Phys. Chem. B* **106**, 7729 (2002)
196. H. Itoh, A. Tahara, K. Naka, Y. Chujo, *Langmuir* **20**, 1972 (2004)
197. C.G. Overberger, Y. Inaki, *J. Polym. Sci., Polym. Chem. Ed.* **17**, 1739 (1979)
198. M.J. Moghaddam, S. Hozumi, Y. Inaki, K. Takemoto, *Polym. J.* **21**, 1739 (1989)
199. M.J. Moghaddam, K. Kanbara, S. Hozumi, Y. Inaki, K. Takemoto, *Polym. J.* **22**, 369 (1990)
200. M.J. Moghaddam, S. Hozumi, Y. Inaki, K. Takemoto, *Polym. J.* **21**, 203 (1989)
201. H. Itoh, K. Naka, Y. Chujo, *J. Am. Chem. Soc.* **126**, 3026 (2004)
202. J.G. Huddleston, H.D. Willauer, R.P. Swatloski, A.E. Visser, R.D. Rogers, *Chem. Commun.* 1765 (1998)
203. C.J. Mathews, P.J. Smith, T. Welton, A.J.P. White, D.J. Williams, *Organometallics* **20**, 3848 (2001)

204. L. Cammarata, S.G. Kazarian, P.A. Salter, T. Welton, *Phys. Chem. Chem. Phys.* **3**, 5192 (2001)
205. S. Carda-Broch, A. Berthod, D.W. Armstrong, *Anal. Bioanal. Chem.* **375**, 191 (2003)
206. R. Tatumi, H. Fujihara, *Chem. Commun.* 83 (2005)
207. K.-S. Kim, D. Demberelnyamba, H. Lee, *Langmuir* **20**, 556 (2004)
208. T. Welton, *Chem. Rev.* **99**, 2071 (1999)
209. J. Dupont, R.F. de Souza, P.A.Z. Suarez, *Chem. Rev.* **102**, 3667 (2002)
210. G.T. Wei, Z.S. Yang, C.Y. Lee, H.Y. Yang, C.R.C. Wang, *J. Am. Chem. Soc.* **126**, 5036 (2004)
211. T. Nakashima, T. Kawai, *Chem. Commun.* 1643 (2005)
212. J. Simard, C. Briggs, A.K. Boal, V.M. Rotello, *Chem. Commun.* 1943 (2000)
213. C.-H. Su, P.-L. Wu, C.-S. Yeh, *Bull. Chem. Soc. Jpn.* **77**, 189 (2004)
214. J.-H. Kim, T.R. Lee, *Chem. Mater.* **16**, 3647 (2004)
215. P.R. Selvakannan, S. Mandel, S. Phadtare, R. Pasricha, M. Sastry, *Langmuir* **19**, 3545 (2003)
216. K. Naka, H. Tanaka, Y. Chujo, *Polym. J.* **39**, 1122 (2007)
217. T. Yonezawa, S. Onoue, N. Kimizuka, *Chem. Lett.* 1172 (2002)
218. A. Larsson, C. Walldal, S. Wall, *Colloids Surf. A, Physicochem. Eng. Asp.* **191**, 65 (1999)
219. Z. Zhong, S. Patskovskyy, P. Bouvrette, J.H.T. Luong, A. Gendanken, *J. Phys. Chem. B* **108**, 4046 (2004)
220. J.N. Cha, H. Birkedal, L.E. Euliss, M.H. Bartl, M.S. Wong, T.J. Deming, G.D. Stucky, *J. Am. Chem. Soc.* **125**, 8285 (2003)
221. V.S. Murthy, J.N. Cha, G.D. Stucky, M.S. Wong, *J. Am. Chem. Soc.* **126**, 5292 (2004)
222. S. Ulrich, M. Seijo, A. Laguecir, S. Stoll, *J. Phys. Chem. B* **110**, 20954 (2006)
223. A. Sehgal, Y. Lalatonne, J.-F. Berret, M. Morvan, *Langmuir* **21**, 9359 (2005)

Nanohybridization of Organic-Inorganic Materials

Muramatsu, A.; Miyashita, T. (Eds.)

2009, XVI, 288 p. 191 illus., 37 illus. in color., Hardcover

ISBN: 978-3-540-92232-2